The relationship between mitochondrial state, ATP hydrolysis, $[Mg^{2+}]_i$ and $[Ca^{2+}]_i$ studied in isolated rat cardiomyocytes

Anne Leyssens, Alex V. Nowicky, Lilian Patterson, Martin Crompton* and Michael R. Duchen†

*Departments of Physiology and *Biochemistry, University College London, Gower Street, London WC1E 6BT, UK*

1. As ATP has a higher affinity for Mg^{2+} than ADP, the cytosolic magnesium concentration rises upon ATP hydrolysis. We have therefore used the Mg^{2+}-sensitive fluorescent indicator Magnesium Green (MgG) to provide an index of changing ATP concentration in single rat cardiomyocytes in response to altered mitochondrial state.

2. In response to FCCP, $[Mg^{2+}]_i$ rose towards a plateau coincident with the progression to rigor, which signals ATP depletion. Contamination of the MgG signal by changes in intracellular free Ca^{2+} concentration (the K_D of MgG for Ca^{2+} is 4·7 μM) was excluded by simultaneous measurement of $[Ca^{2+}]_i$ and $[Mg^{2+}]_i$ in cells dual loaded with fura-2 and MgG. The response to FCCP was independent of external Mg^{2+}, confirming an intracellular source for the rise in $[Mg^{2+}]_i$.

3. Simultaneous measurements of mitochondrial NAD(P)H autofluorescence and mitochondrial potential ($\Delta\psi_m$; JC-1 fluorescence) and of autofluorescence and MgG allowed closer study of the relationship between $[Mg^{2+}]_i$ and mitochondrial state. Oligomycin abolished the FCCP-induced rise in $[Mg^{2+}]_i$ without altering the change in autofluorescence. Thus, the rise in $[Mg^{2+}]_i$ in response to FCCP is consistent with the release of intracellular Mg^{2+} following ATP hydrolysis by the mitochondrial F_1F_0-ATPase.

4. The rise in $[Mg^{2+}]_i$ was correlated with cell-attached recordings of ATP-sensitive K^+ channel (K_{ATP}) activity. In response to FCCP, an increase in K_{ATP} channel activity was seen only as $[Mg^{2+}]_i$ reached a plateau. In response to blockade of mitochondrial respiration and glycolysis with cyanide (CN^-) and 2-deoxyglucose (DOG), $[Mg^{2+}]_i$ rose more slowly but again K_{ATP} channel opening increased only when $[Mg^{2+}]_i$ reached a plateau and the cells shortened.

5. Oligomycin decreased the rate of rise of $[Mg^{2+}]_i$, delayed the onset of rigor and increased the rate of mitochondrial depolarization in response to CN^-–DOG. Thus, with blockade of mitochondrial respiration, $\Delta\psi_m$ is maintained by the mitochondrial F_1F_0-ATPase at the expense of ATP reserves.

6. In response to CN^-–DOG, the initial rise in $[Mg^{2+}]_i$ was accompanied by a small rise in $[Ca^{2+}]_i$. After $[Mg^{2+}]_i$ reached a plateau and rigor developed, $[Ca^{2+}]_i$ rose progressively. On reperfusion, in hypercontracted cells, $[Ca^{2+}]_i$ recovered before $[Mg^{2+}]_i$ and $[Ca^{2+}]_i$ oscillations were sustained while $[Mg^{2+}]_i$ decreased. Thus on reperfusion, full recovery of $[ATP]_i$ is slow, but the activation of contractile elements and the restoration of $[Ca^{2+}]_i$ does not require the re-establishment of millimolar concentrations of ATP.

During a limited period of anoxia or ischaemia, changes in cell function may be fully reversible. However, after a time that varies with different tissues, changes in cell function become irreversible and are associated with damage, and, eventually, with cell death. The factors that determine cell fate during or following such episodes are poorly understood. Adenosine-5′-triphosphate (ATP) plays a central role in the cellular economy; thus a failure to maintain cytosolic [ATP]

† To whom correspondence should be addressed.

may underpin many of the changes that take place during periods of metabolic distress. Since mitochondria play a central role in the onset and evolution of ischaemic damage to the heart and in its potential recovery during reperfusion, measurements of the mitochondrial redox state, reflected by changes in NAD(P)H autofluorescence (Eng, Lynch & Balaban, 1989), and of the mitochondrial membrane potential ($\Delta\psi_m$) (Duchen, McGuinness, Brown & Crompton, 1993; Di Lisa *et al.* 1995), can give valuable information about mitochondrial function in these conditions. The recovery of single cardiomyocytes on reperfusion is also largely dependent on the changes in $[Ca^{2+}]_i$ during the preceding ischaemic period (Miyata, Lakatta, Stern & Silverman, 1992). However, previous studies only provide circumstantial evidence for the relationship in single cardiomyocytes between $[ATP]_i$, mitochondrial function and $[Ca^{2+}]_i$. We have been concerned to find ways to monitor changes in $[ATP]_i$ in single cells so that it is possible (i) to correlate changes in other aspects of cell function and cell biochemistry with ATP depletion, and (ii) to assess the factors that determine the rate of ATP depletion during ischaemia and the rate of repletion on reperfusion.

Direct measurements of $[ATP]_i$ are feasible in single cells, using the chemiluminescent couple, luciferin–luciferase (Bowers, Allshire & Cobbold, 1993). However, this approach is not without its problems. Luciferase must be microinjected into cells. The luciferin–luciferase reaction requires oxygen, and so it is not practical to use this approach to study changes in $[ATP]_i$ with true hypoxia or anoxia. The sensitivity of the probe – the luciferase signal saturates at 3–5 mM ATP (Bowers *et al.* 1993) – limits its usefulness to establish changes in the millimolar range. Consequently, during or after a metabolic insult, the initial fall of $[ATP]_i$ from or the full recovery to its control value of up to 10 mM (Geisbuhler, Altschuld, Trewyn, Ansel, Lamka & Brierly, 1984) may not be detected. Changes in the signal are not always easy to interpret, and since luminescence is highly pH dependent, it may not simply reflect $[ATP]_i$ alone (Bowers *et al.* 1993). In particular, relevant to the objective of the present study, it is difficult to make measurements of luciferase chemiluminescence simultaneously with fluorescence measurements from other probes to correlate changes in $[ATP]_i$ with other physiological variables that are changing during and after an ischaemic period.

In isolated hearts, total magnesium levels are not significantly altered during myocardial ischaemia followed by reperfusion (Kirkels, van Echtfeld & Ruigrok, 1989). However, NMR studies have shown that intracellular free magnesium ($[Mg^{2+}]_i$) rises as $[ATP]_i$ falls (Murphy, Steenbergen, Levy, Raju & London, 1989). This is likely to reflect the fact that a large part of the intracellular pool of Mg^{2+} is present as MgATP. As the affinity of ATP for Mg^{2+} is about tenfold greater than that of ADP, ATP hydrolysis leads to a rise in $[Mg^{2+}]_i$. The intracellular Mg^{2+} concentration typically more than doubles from its basal level of approximately 0·8 mM under conditions in which $[ATP]_i$ is expected to fall from its control level of 5–10 mM towards total ATP depletion, implying that part of the Mg^{2+} liberated during ATP hydrolysis must be bound to other intracellular components. Although the precise relationship between changes in $[Mg^{2+}]_i$ and $[ATP]_i$ remains to be elucidated in single cells, Silverman *et al.* (1994), using the fluorescent Mg^{2+}-sensitive indicator mag-indo-1, demonstrated that measurements of $[Mg^{2+}]_i$ in single cardiomyocytes, although indirect, may give a very sensitive measure of the rate of change of $[ATP]_i$ within metabolically compromised single cardiomyocytes. This study also confirmed that in cell suspensions rapid decreases in $[ATP]_i$, as measured with the chemiluminescent luciferin–luciferase assay, are accompanied by a rise in $[Mg^{2+}]_i$.

In the present study, we have used the new probe Magnesium Green (MgG) to follow changes in $[Mg^{2+}]_i$ with changing metabolic state in single cardiomyocytes isolated from rat heart. The spectral properties of the dye and the use of the appropriate optical arrangements allow measurements of $[Mg^{2+}]_i$ to be combined with measurements of $[Ca^{2+}]_i$, using fura-2 or with assessments of redox state measured as NAD(P)H autofluorescence. Combining measurements of NAD(P)H autofluorescence with measurements of $\Delta\psi_m$ (using the fluorescent probe 5,5′,6,6′-tetrachloro-1,1′,3,3′-tetraethylbenzimidazolylcarbocyanine iodide (JC-1)) on the one hand, and with $[Mg^{2+}]_i$ measurements on the other, give further insight into the relationship between changes in mitochondrial respiration, $\Delta\psi_m$ and $[ATP]_i$. In cardiomyocytes, ATP depletion also leads to the opening of K^+ channels normally kept closed by ATP (K_{ATP} channels) (Noma, 1983). In isolated patches of membrane, these channels open as ATP falls below about 1 mM, with a K_D of 20–100 μM (Lederer & Nichols, 1989). We have also used measurements of the activity of these channels to identify the relative range of the MgG signals as a reflection of ATP depletion and thus to obtain more insight into the relationship between changes in $[Mg^{2+}]_i$ and $[ATP]_i$.

In order to assess the usefulness of MgG as an indicator for changes in $[ATP]_i$, we have used the mitochondrial uncoupler carbonyl cyanide *p*-trifluromethoxyphenylhydrazone (FCCP) to induce rapid ATP depletion. We have also examined the same set of variables under conditions in which both mitochondrial and glycolytic metabolism are inhibited, using the now standard combination of cyanide (CN^-) and 2-deoxyglucose (DOG).

Preliminary accounts of these results have been communicated to The Physiological Society (Leyssens & Duchen, 1994; Leyssens, Nowicky, Patterson, Crompton & Duchen, 1995).

METHODS

Preparation of rat cardiomyocytes

Isolation procedure. Isolated rat cardiomyocytes were prepared essentially as previously described (Nazareth, Yafei & Crompton, 1991). Sprague–Dawley rats (mean weight, 250 g) were killed by cervical dislocation. The heart was excised, attached to a Langendorff column, and perfused with a Ca^{2+}-free physiological salt solution containing (mM): 118 NaCl, 4·8 KCl, 1·2 KH_2PO_4, 1·2 $MgSO_4$, 25 $NaHCO_3$, and 11 glucose (solution A); maintained at 37 °C and equilibrated with 95% O_2–5% CO_2 giving a pH of 7·4. The heart was first rinsed with approximately 40 ml perfusate and then 50 μg (100 ml)$^{-1}$ collagenase (Type II, Worthington Biochemical Co.) and 30 μg (100 ml)$^{-1}$ hyaluronidase (Type I, Sigma) were added. Thereafter the effluent was recycled. After 10 min the Ca^{2+} concentration was raised in three stages to a final concentration of 0·5 mM. After another 8–10 min, the ventricles were excised and minced and then incubated for 30 min with 25 ml of the recycling medium. The flask was shaken at 75 cycles min^{-1}. The resulting material was triturated, filtered through a mesh, and then centrifuged (for 90 s at 30 *g*). The pellets were washed twice by resuspension and centrifugation and finally resuspended in a Hepes-buffered saline (solution B) containing (mM): 118 NaCl, 4·8 KCl, 25 Hepes, 1·2 $MgSO_4$, 1 $CaCl_2$, 1·2 KH_2PO_4, 11 glucose and 1% bovine serum albumin (BSA).

Preparation of cardiomyocyte culture. Since the isolation procedure was non-sterile, the cardiomyocytes were treated for 10 min with 50 μg ml^{-1} gentamicin in solution B. They were centrifuged (for 90 s at 30 *g*) and washed three times before resuspension at a density of approximately 2×10^5 cells ml^{-1} in M-199 medium (Sigma) supplemented with 0·2% BSA (medium A). Subsequently the cells were plated on sterile laminin-coated (1 μg cm^{-2}) coverslips (24 mm) in 35 mm sterile Petri dishes and kept in an incubator at 37 °C under an atmosphere of 5% CO_2–95% air. After a 3 h attachment period, medium A was added to the Petri dish. Since only intact cells attach to the coverslip, a preparation of almost 100% intact (rod-shaped) cells was obtained. Medium A was renewed every day and the cardiomyocytes were kept in culture for up to 4 days. Over this time the cells preserved their normal ultrastructure and showed no signs of dedifferentiation. In the present study, no statistically significant differences were apparent with time in culture with respect to the electrophysiological and microfluorimetric variables studied.

Experimental arrangement for fluorescence measurements

Cells were loaded with Magnesium Green (MgG) in the AM ester form (5 μM) with the addition of Pluronic (2%) for 30 min at room temperature (18–22 °C). In some experiments, cells were also loaded with fura-2 (AM ester, 5 μM), which was introduced at the same time. The cells were washed in a physiological saline (solution B, above) and placed into a home-made chamber on the stage of an inverted epifluorescence microscope. Fluorescence was elicited by illumination with a 75 W xenon arc lamp via a filter wheel (Cairn Research, Faversham, Kent, UK) that rotated at 12 Hz allowing rapid sequential excitation of fluorescence through 10 nm bandpass filters centred at 340, 360, 380 and 490 nm. Cells were also transilluminated with red light (> 600 nm) from a tungsten–halogen lamp. A ×40 oil immersion quartz objective lens (numerical aperture, 1·3) was used to maximize signal collection and the light path for the emitted fluorescence signal involved a long-pass 600 nm dichroic mirror in front of a videocamera to allow observation of the transilluminated image of the cell simultaneously with the collection of the fluorescence signal. The fluorescence signals were measured using a photomultiplier tube (PMT) after passing through a 530 ± 10 nm bandpass filter. The excitation spectra of MgG (490 nm) and fura-2 (340 and 380 nm) are sufficiently distinct to allow separate excitation while the emission spectra overlap sufficiently to allow measurement of both fluorescence signals with a single detector.

Simultaneous measurements of MgG and NAD(P)H autofluorescence required a slightly more complex optical arrangement. In this case, a double reflectance band dichroic mirror (Chroma Technologies) was used in the epifluorescence light path to allow illumination with light at 360 nm (for excitation of NAD(P)H) and at 490 nm (for MgG) with transmission bands from ~400–480 nm and then above 510 nm to allow simultaneous collection of both the NAD(P)H autofluorescence (with a peak at 450 nm) and the MgG signal (with a peak at 530 nm). The fluorescence signals from the two excitation bands were collected with two photomultiplier tubes separated by a dichroic mirror at 510 nm. A 450 nm wideband (±40 nm) filter was used in front of the PMT used to measure the autofluorescence signal, while the usual 530 nm filter was used to collect the signal from MgG fluorescence.

In another series of experiments, NAD(P)H autofluorescence measurements were combined with simultaneous measurements of $\Delta\psi_m$ using the indicator JC-1 (5,5′,6,6′-tetrachloro-1,1′,3,3′-tetraethylbenzimidazolylcarbocyanine iodide; Molecular Probes) (Reers, Smith & Chen, 1991; Duchen *et al.* 1993). To this end, cells were loaded with 10 μM JC-1 for 10 min at 37 °C. JC-1 in its monomeric form emits fluorescence at 530 nm when excited at 490 nm. As a lipophilic cation, it partitions into mitochondria where it forms 'J' complexes which emit fluorescence at 590 nm (Reers *et al.* 1991). Depolarization of $\Delta\psi_m$ leads to redistribution of the dye with the disaggregation of J complexes, and so causes a decrease in the signal at 590 nm and an increase at 530 nm (Duchen *et al.* 1993; Di Lisa *et al.* 1995). In order to monitor the JC-1 fluorescence and NAD(P)H autofluoresence signals simultaneously, we used the emission band at 530 nm to signal mitochondrial depolarization, using the same optical arrangement as used for MgG and autofluorescence (see above).

Fluorescence signals were digitized to 12-bit resolution at 5–10 Hz and stored on disk using a Tecmar Labmaster A-D converter in combination with LabTech Notebook Software (Adept Scientific, Letchworth, Herts, UK).

Calibration of the fluorescence signals

NAD(P)H autofluorescence measurements and JC-1 fluorescence measurements (at 530 nm) are presented as a percentage change compared with control.

Fura-2 fluorescence signals were calibrated in terms of $[Ca^{2+}]_i$ using the equation:

$$[Ca^{2+}]_i = K_D\beta(R_{max} - R)/(R - R_{min}),$$

with a dissociation constant (K_D) of 224 nM (Grynkiewicz, Poenie & Tsien, 1985), where R_{min} and R_{max} are minimum and maximum fluorescence ratios, respectively, and β is the value of the ratio of the 380 nm signal in zero Ca^{2+} divided by that in saturating $[Ca^{2+}]_i$. R_{max} was obtained by damaging the cell with a pipette. This elevates $[Ca^{2+}]_i$ to a saturating level without loss of dye during the first minute. In order to estimate R_{min}, cells were bathed in Ca^{2+}-free saline (containing 1 mM EGTA) and were further loaded for 20 min with the Ca^{2+} chelator 1,2-bis(2-aminophenoxy)ethane-*N,N,N′,N′*-tetraacetic acid-acetoxymethyl ester (BAPTA AM; 10 μM).

Calibration of the MgG signal to yield true values of free $[Mg^{2+}]_i$ were fraught with difficulties. Firstly, use of a single wavelength dye brings the usual problems of calibration with variable loading and variable cell size. Attempts to vary the signal systematically using combinations of ionophore and variable external $[Mg^{2+}]_i$ to indicate maximal and minimal signals proved unusually difficult. The ionophores A23187 and ionomycin both admit Mg^{2+}, but also act as mitochondrial uncouplers, which raise $[Mg^{2+}]_i$ (see below) and so the uncoupler FCCP was applied first to establish the part of the signal related to the uncoupling action of the ionophores. Further, as the MgG signal is significantly sensitive to $[Ca^{2+}]_i$ in the micromolar range, attempted calibrations were performed in Ca^{2+}-free buffers after loading cells with BAPTA AM (10 μM) to exclude contributions of internal Ca^{2+} pools to the signal. Application of A23187 in a Mg^{2+}-free saline (with 1 mM EGTA and 1 mM EDTA) then caused a decline in the signal, but equilibration was very slow. Similar problems are described using mag-indo-1 (Silverman *et al.* 1994) although some of these problems are mitigated by the use of a ratiometric indicator. It seems very difficult to obtain useful numbers that can give secure calibrations of the Mg^{2+} signal, and so we have presented all our data in terms of a percentage change in signal.

Patch clamp experiments

Cell-attached patch recordings were made using conventional techniques with a List EPC-7 amplifier from cells loaded with MgG AM. Data were stored on videotape (PCM-8, Medical Systems Corp., Greenvale, NY, USA) and digitized off-line for analysis using the pCLAMP 6 software suite (Axon Instruments, Foster City, CA, USA). Channel activity was expressed as NP_o, where N represents the number of channels in the patch and P_o the probability of each channel being open. Fluorescence signals were re-sampled and analysed as described above. A trigger signal allowed correlation between the electrophysiological and fluorescence signals.

Drugs and solutions

For most experiments, cells were bathed in a solution containing (mM): 118 NaCl, 4·8 KCl, 25 Hepes, 1·2 $MgSO_4$, 2 $CaCl_2$, 1·2 KH_2PO_4, and 11 glucose; pH adjusted to 7·4 with NaOH. During reperfusion, i.e. during washout of CN^-–DOG, 5 mM sodium pyruvate was added to the bath solution. In some experiments $CaCl_2$ was omitted from the bath solution and 1 mM EGTA added with appropriate pH correction (the Ca^{2+}-free saline solution). Cells permeabilized with digitonin and/or Triton X-100 were bathed in a buffer with the following composition (mM): 90 KCl, 10 NaCl, 30 Pipes, 1 EGTA, 1 $MgSO_4$, 4·5 MgATP, and 10 creatine phosphate; we adjusted $[Mg^{2+}]$ to 1 mM, close to estimations of basal (Silverman *et al.* 1994) and mitochondrial $[Mg^{2+}]$ (Jung & Brierly, 1994). Patch pipettes were filled with a solution (see Weiss & Lamp, 1989) containing (mM): 150 KCl, 5 Hepes, and 4–6 Ca^{2+}; pH adjusted to 7·4 with KOH.

Drugs used included carbonyl cyanide *p*-trifluoromethoxy-phenylhydrazone (FCCP) at 1–2 μM, cyanide (CN^-; sodium salt) at 2·5 mM, 2-deoxyglucose (DOG) at 20 mM, oligomycin (mixture of types A, B and C) at 5 μg ml^{-1}. Most drugs were applied locally under pressure ejection from micropipettes, thus limiting exposure of most cells in the bath to potentially toxic compounds. Oligomycin was added to the bath solution. In some cases cells were loaded with the AM ester of the Ca^{2+} buffer BAPTA, using the same protocols as used to load fura-2. All fluorescent probes and BAPTA AM were obtained from Molecular Probes, and all other drugs were from Sigma.

Statistics

All results are presented as means ± S.E.M. Unless otherwise stated, statistical discriminations were performed with Student's unpaired two-tailed t test, and $P < 0·05$ was regarded as significant.

RESULTS

MgG responds primarily to changes in $[Mg^{2+}]_i$ and reflects changes in $[ATP]_i$

One of the problems associated with the use of Mg^{2+}-sensitive fluorescent indicators is that they all show a significant sensitivity to $[Ca^{2+}]_i$. The probe MgG has a reported K_D for Ca^{2+} of 4·7 μM while the K_D for Mg^{2+} is 0·9 mM. This means that changes in fluorescence of the Mg^{2+} probe must be interpreted with caution, especially under conditions in which $[Ca^{2+}]_i$ is known to rise. In an attempt to resolve this issue, cells were dual loaded with both the Ca^{2+} indicator fura-2 and MgG.

Figure 1*A* shows the fluorescence signals obtained, at room temperature, from the two indicators; firstly a rise in $[Ca^{2+}]_i$ in response to brief applications of caffeine and then to the application of the uncoupler FCCP. Caffeine evoked a transient rise in $[Ca^{2+}]_i$ as expected, with minimal disturbance of the MgG signal. Application of FCCP produced a rapid increase in MgG signal followed by a slower rise to a plateau. Saturation of the MgG signal during the plateau phase can be excluded since damaging the cells with a pipette in a high $[Mg^{2+}]$ solution (20 mM) could further increase the MgG signal (from 180 ± 6 to 205 ± 8%, $n = 5$, $P < 0·05$). Cell shortening to 55 ± 5% ($n = 9$) of the original cell length, a rigor contracture due to the depletion of cellular ATP, occurs during the plateau phase. The mean rise in MgG in response to FCCP was 177 ± 6% ($n = 9$), while the mean time to cell shortening was 175 ± 36 s ($n = 9$), showing a large variability in the rate of ATP depletion between individual cells. Raising the bath temperature to 34 °C did not significantly alter the mean rise in MgG fluorescence (167 ± 7%, $n = 7$) nor the mean time to cell shortening (107 ± 11 s, $n = 7$) in response to FCCP.

The rise in the MgG signal in response to FCCP, followed by cell shortening, was not significantly different following the removal of external Ca^{2+} (mean rise in MgG fluorescence, 187 ± 9%, $n = 13$; mean time to cell shortening, 160 ± 27 s, $n = 13$); neither was a statistically significant difference found when intracellular Ca^{2+} was additionally buffered using BAPTA loaded as the AM ester (shown in Fig. 1*B*) (mean MgG fluorescence rise, 160 ± 4%, $n = 7$; mean time to cell shortening, 89 ± 10 s, $n = 7$). As a control it is shown that in this condition depolarizing the plasma membrane by applying 50 mM K^+ does not cause a rise in $[Ca^{2+}]_i$.

Thus, the change in MgG fluorescence in response to the uncoupler seems to be unequivocally due to a change in $[Mg^{2+}]_i$, without significant contamination from changes in

$[Ca^{2+}]_i$. Furthermore, in agreement with an earlier study by Haworth, Hunter & Berkhof (1981), the rate of onset of rigor is independent of external Ca^{2+}. The source of the rise in $[Mg^{2+}]_i$ was further examined by looking at the responses to FCCP in the absence of external Ca^{2+} and in the absence of external Mg^{2+} (with internal Ca^{2+} buffered using BAPTA AM). The response to FCCP was essentially unchanged (mean rise in MgG fluorescence, $177 \pm 4\%$, $n = 6$; mean time to cell shortening, 86 ± 10 s, $n = 7$), suggesting that the source of Mg^{2+} is intracellular and that Mg^{2+} losses from the cell within this time frame are negligible. This is clearly compatible with the supposition that the $[Mg^{2+}]_i$ rises as a result of release from ATP hydrolysis.

Changes in MgG signal in response to FCCP are consistent with cellular ATP depletion due to ATP hydrolysis by the mitochondrial F_1F_0-ATPase

The major changes in oxidative phosphorylation in response to an uncoupler are due to depolarization of the

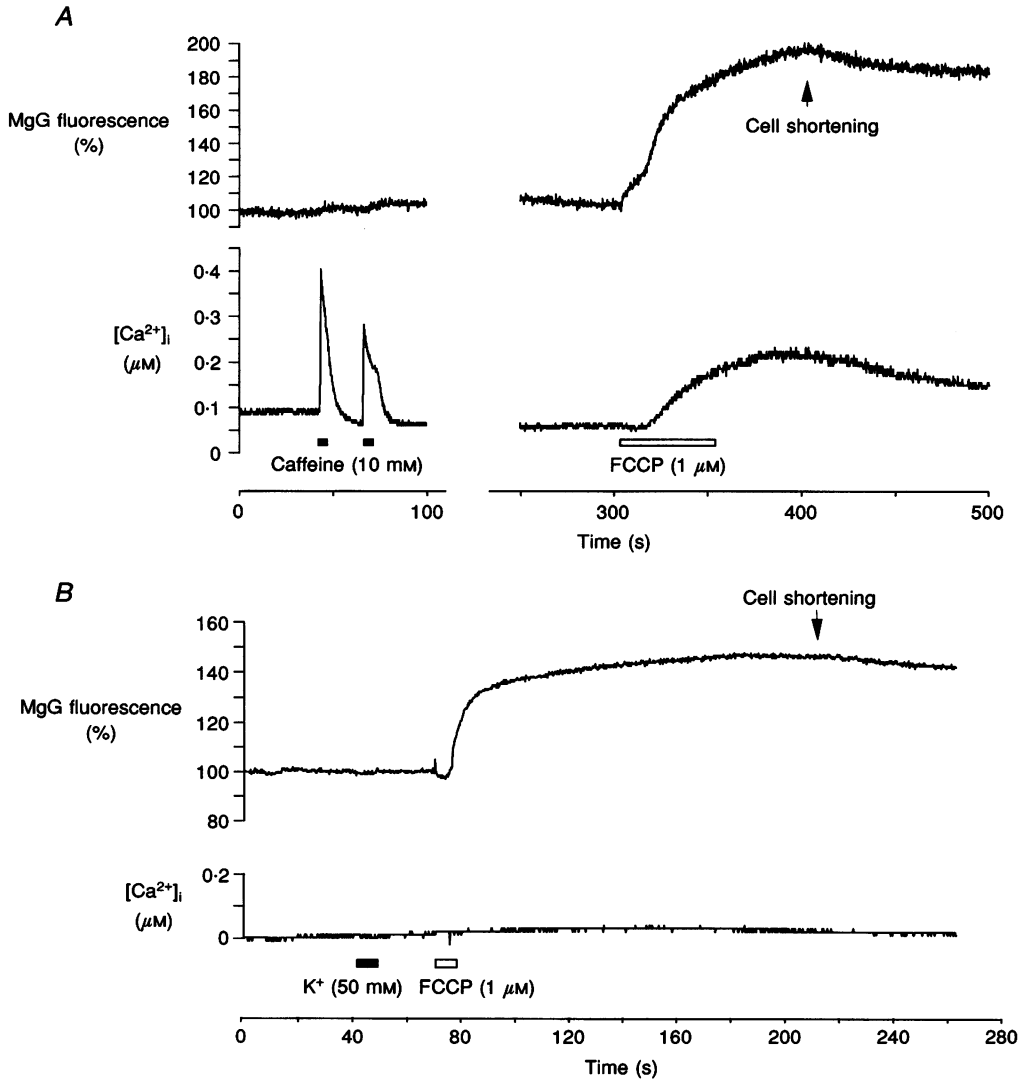

Figure 1. Time course of changes in MgG fluorescence and $[Ca^{2+}]_i$ in response to FCCP in the presence and absence of external Ca^{2+}

A, fluorescence signals obtained from a cardiomyocyte loaded with both MgG (upper trace) and fura-2 (lower trace). Two applications of caffeine as indicated (10 mM; filled bar) caused rapid, large $[Ca^{2+}]_i$ transients, but a negligible change in the MgG signal. Shortly afterwards, application of FCCP (1 μM) for the period indicated by the open bar caused a large increase in the MgG signal, with a small slow increase in the fura-2 ratio. *B*, a record from another cell which was also loaded with BAPTA AM to buffer any Ca^{2+} released from internal stores, and was superfused continuously with a Ca^{2+}-free saline (including 1 mM EGTA). Depolarization of the cell with 50 mM K^+ (filled bar) had no effect on either $[Ca^{2+}]_i$ or the MgG signal. Application of FCCP (1 μM; open bar) caused a large and rapid increase in the MgG signal to a new plateau level, without any change in $[Ca^{2+}]_i$. These experiments were performed at room temperature.

mitochondrial membrane potential. In order to examine the time course of the mitochondrial response to FCCP more precisely, the emission of the potentiometric probe JC-1 at 530 nm was measured simultaneously with NAD(P)H autofluorescence. The responses to FCCP are illustrated in Fig. 2*A*. Brief application of FCCP caused a rapid increase in the JC-1 signal at 530 nm (mean increase to 176 ± 17%, $n = 4$), closely followed by a decrease in the NAD(P)H autofluorescence signal (mean decrease to 52 ± 6%, $n = 4$). Figure 2*B* shows a plot of NAD(P)H fluorescence as a function of the JC-1 signal, showing clearly that the mitochondrial depolarization precedes the decrease in autofluorescence, signalling an increased rate of respiration. Thus these signals illustrate the relationship between mitochondrial depolarization and the increased rate of NAD(P)H oxidation and demonstrate that changes in NAD(P)H autofluorescence can be used as an internal standard for the uncoupling effect of FCCP.

Thus, FCCP stimulates mitochondrial respiration, and the fluorimetry allows direct assessment of the rates of change of these variables. The depolarization of $\Delta\psi_m$ in response to

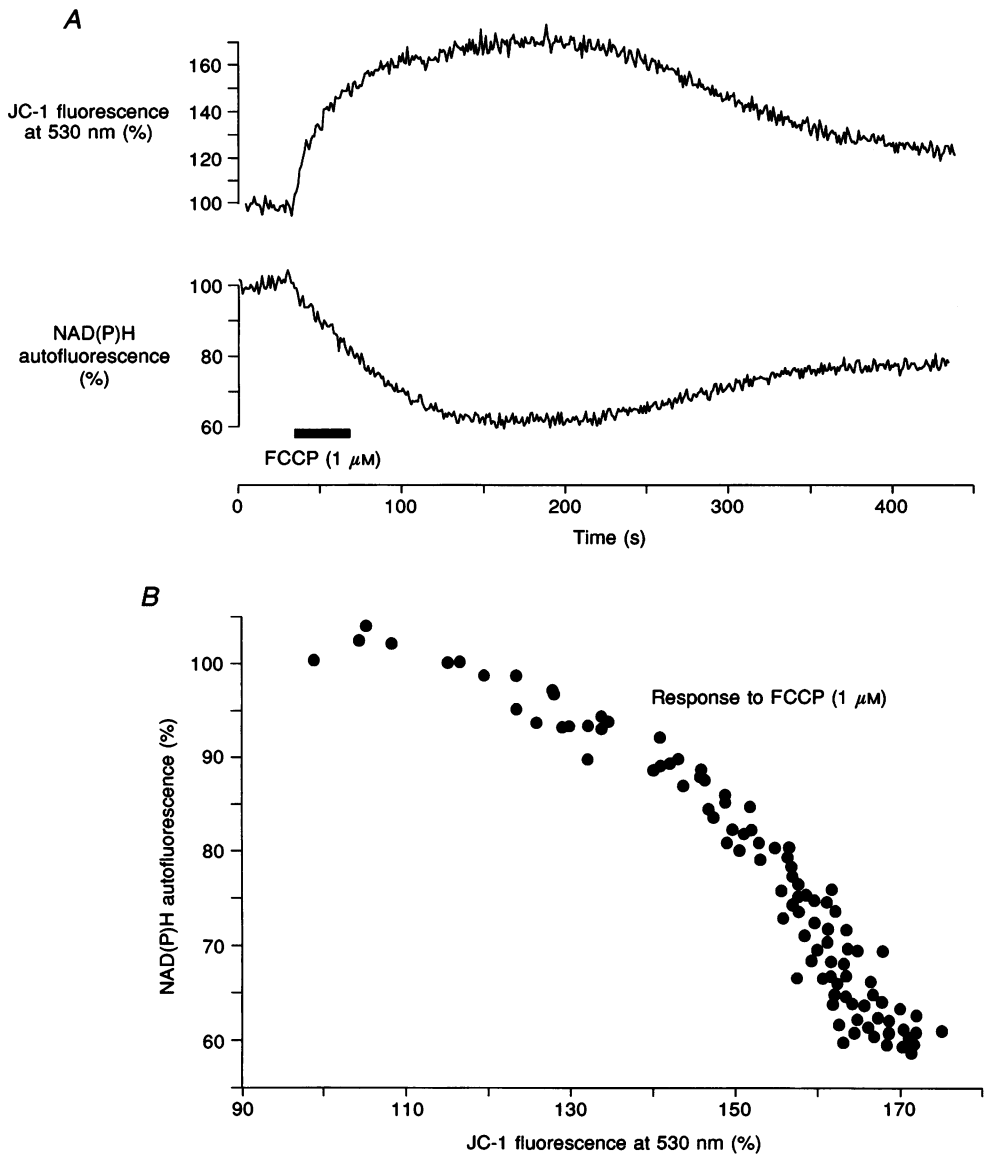

Figure 2. Relationship between changes in JC-1 fluorescence and NAD(P)H autofluorescence in response to FCCP

A, simultaneous measurements of JC-1 fluorescence (measured at 530 nm) (upper trace) and autofluorescence primarily derived from mitochondrial NAD(P)H (lower trace). Application of FCCP (1 μM; filled bar) caused an increase in the JC-1 signal, indicating mitochondrial depolarization, and the NAD(P)H autofluorescence decreased, reflecting an increased rate of substrate oxidation by the respiratory chain. *B*, the NAD(P)H fluorescence signal is plotted as a function of the JC-1 signal, showing that the mitochondrial depolarization precedes the decrease in autofluorescence. These experiments were performed at room temperature.

FCCP is also expected to promote reversal of the mitochondrial F_1F_0-ATP synthase, which now acts as a proton translocating ATPase. The onset of rigor due to uncoupling of mitochondrial respiration can be prevented with oligomycin, a potent inhibitor of the F_1F_0-ATPase (Haworth *et al.* 1981). Therefore the rate of ATP depletion in response to the uncoupler is largely determined by mitochondrial ATP hydrolysis. This is further demonstrated in the experiment shown in Fig. 3 in which NAD(P)H autofluorescence was now measured simultaneously with the MgG fluorescence. The experiments were performed in Ca^{2+}-free saline. When cells were bathed in 5 μg ml^{-1} oligomycin the response to FCCP was almost completely abolished (Fig. 3*B*), with a mean change to only 107 ± 1% ($n = 6$) compared with 158 ± 3% ($n = 13$) in the absence of oligomycin. However, as expected, the decrease in NAD(P)H

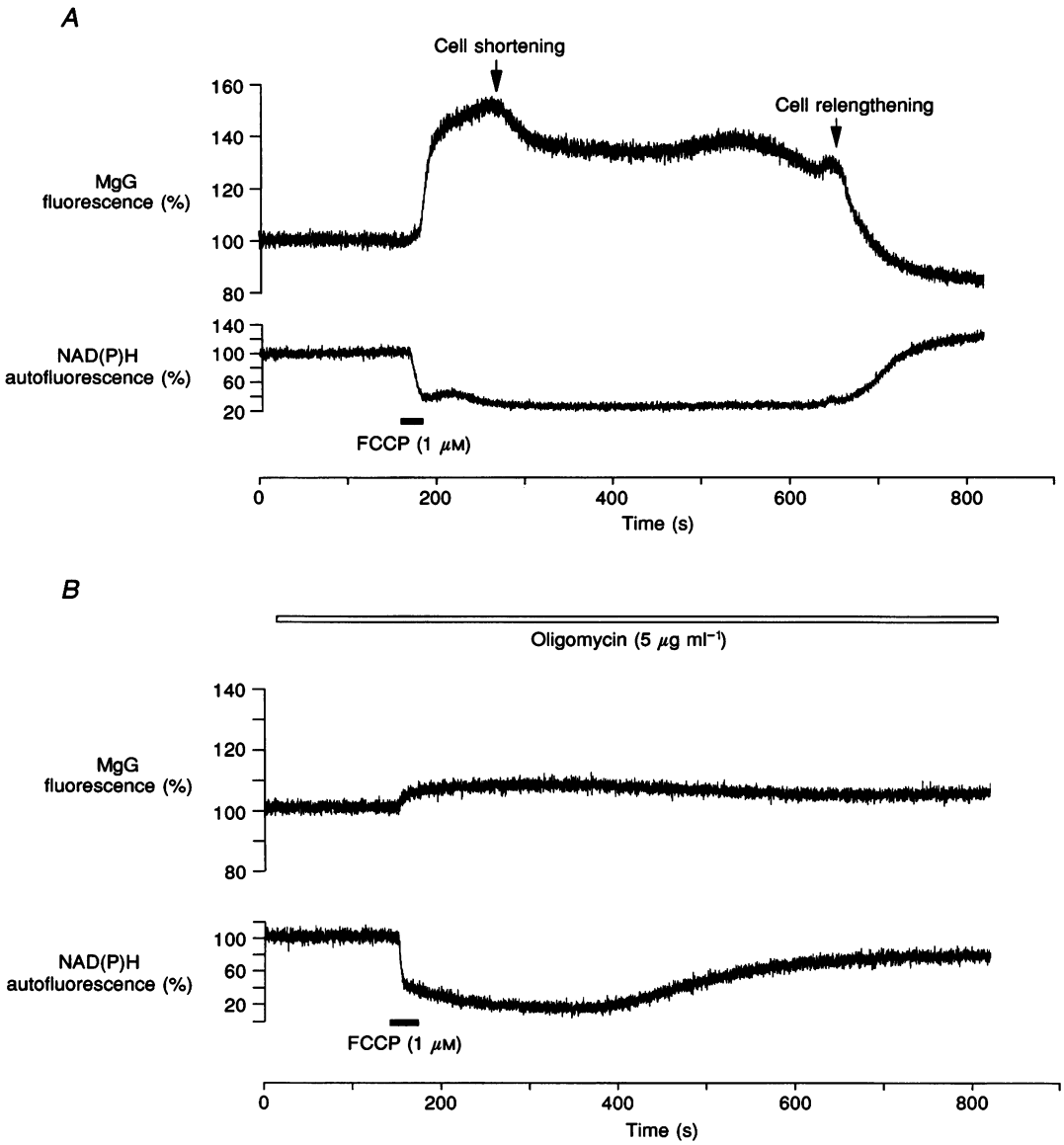

Figure 3. Time course of changes in MgG fluorescence and NAD(P)H fluorescence in response to FCCP in the absence and presence of oligomycin

Simultaneous recordings of MgG fluorescence (upper trace) and NAD(P)H autofluorescence (lower trace) from a cardiomyocyte bathed in Ca^{2+}-free saline at room temperature. *A*, application of FCCP (1 μM; filled bar) caused a rapid rise in the MgG and a rapid fall in the autofluorescence signal. The cell went into rigor as the MgG signal reached a plateau. After a period of about 6 min, the FCCP washed out, the cell relengthened, and the MgG signal recovered more slowly towards the control level. The recovery of the autofluorescence and MgG signals were coincident. The records in *B* show the result of the same experiment, but in the presence of oligomycin (5 μg ml^{-1}). The change in the autofluorescence signal in response to FCCP served as an internal control, confirming the efficacy of the drug in depolarizing the mitochondria and promoting rapid substrate oxidation, while the rise in $[Mg^{2+}]_i$ was largely suppressed.

fluorescence in response to FCCP was similar in the presence (mean decrease to 36 ± 4%, $n = 6$) and absence (mean decrease to 35 ± 4%, $n = 13$) of oligomycin confirming the efficacy of FCCP when the rise in $[Mg^{2+}]_i$ was suppressed. Similar results were obtained from paired experiments in which the (reversible) response to FCCP was followed by a second application in the presence of oligomycin on the same cell. In these, oligomycin substantially reduced the rise in MgG fluorescence from 154 ± 2 to 106 ± 2% ($n = 3$) while the decrease in NAD(P)H autofluorescence was not significantly altered (46 ± 4 and 33 ± 8%, respectively). Oligomycin also inhibited the increase in MgG fluorescence (to 110 ± 2%, $n = 4$) and cell shortening in response to FCCP when the cells were bathed in Ca^{2+}-containing saline.

Note that recovery of the cell following washout of FCCP, was associated with relengthening – signalling the recovery of ATP synthesis and relief of the rigor contracture – and with recovery of both the autofluorescence and MgG signals (Fig. 3*A*).

In addition to these responses, we consistently found that the MgG signal fell slightly to a new level at the time of rigor. Relengthening of the cell on recovery was also invariably preceded by a transient increase in the MgG signal.

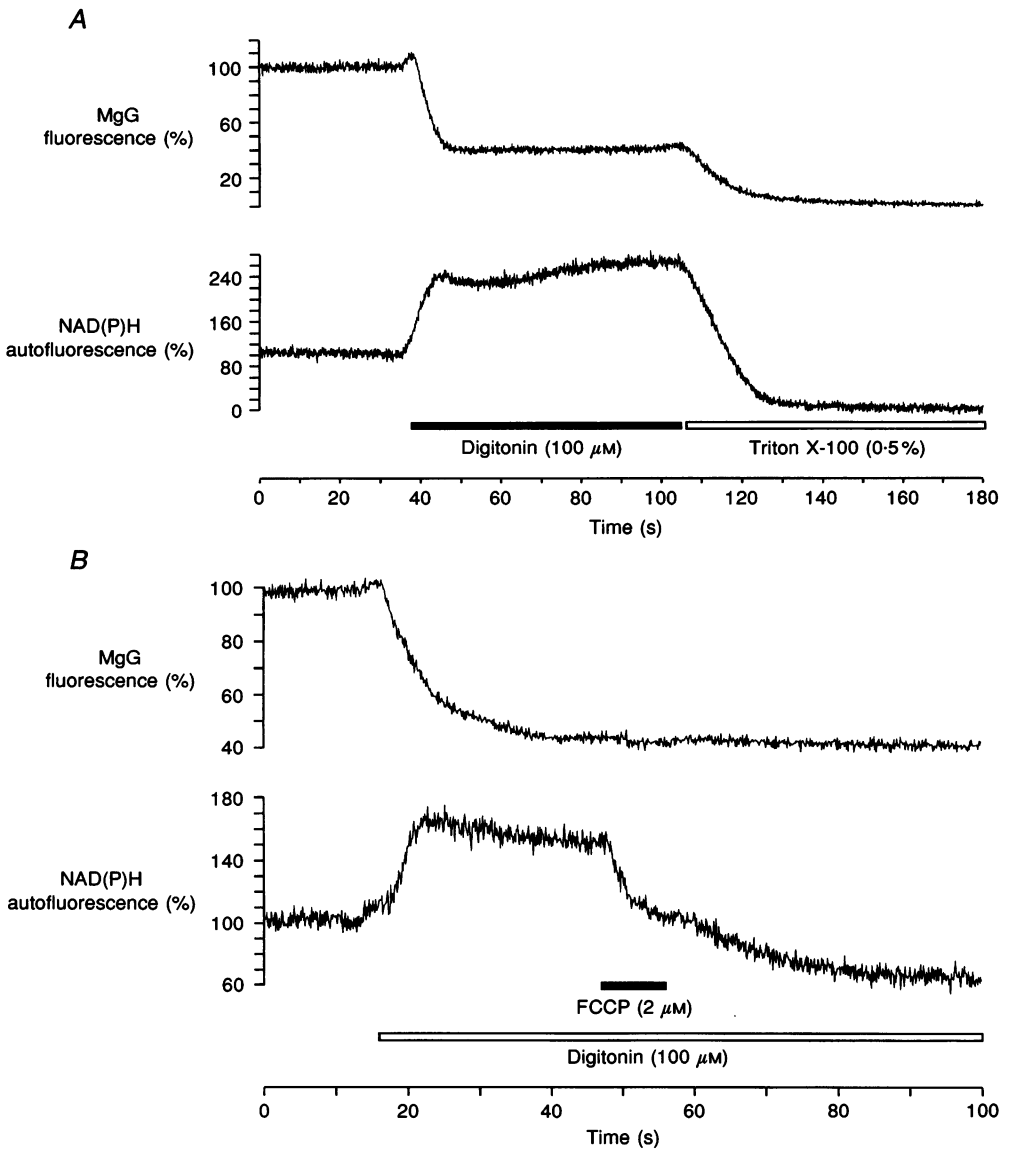

Figure 4. Compartmentalization of the MgG probe

Simultaneous recordings of MgG fluorescence (upper trace) and NAD(P)H autofluorescence (lower trace) were made from single cardiomyocytes bathed in a pseudointracellular saline (see Methods). *A*, the result of consecutive application of digitonin (100 μM; filled bar) and Triton X-100 (0·5%; open bar). *B*, after permeabilization of the plasma membrane with 100 μM digitonin (open bar), FCCP (2 μM; filled bar) still decreased the NAD(P)H autofluorescence, confirming that the mitochondria and the respiratory chain were intact. The experiments were performed at room temperature.

Intracellular distribution and pH sensitivity of MgG

In order to determine the distribution of MgG in intracellular compartments, cells loaded with MgG were permeabilized using digitonin which permeabilizes all cell membranes except mitochondrial membranes. NAD(P)H autofluorescence was monitored simultaneously to assess mitochondrial integrity. Digitonin at 100 μM, which permeabilizes both plasma membrane and sarcoplasmic (SR) or endoplasmic reticular membranes (Roe, Lemasters & Herman, 1990), caused a rapid fall in the MgG signal to a

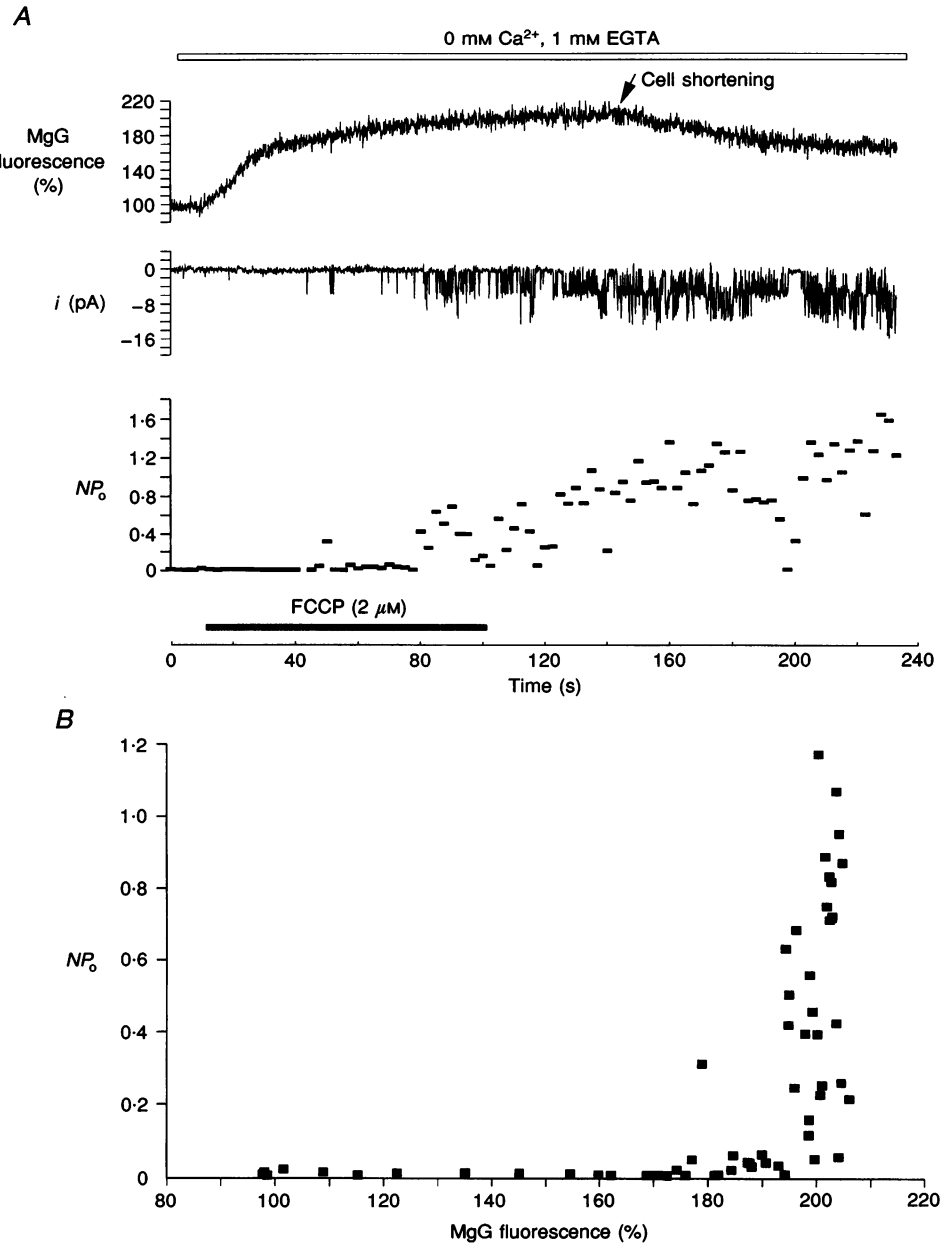

Figure 5. Relationship between changes in MgG fluorescence and K_{ATP} channel activity after the application of FCCP

A, simultaneous measurements of MgG fluorescence (upper trace) and channel activity (middle trace) recorded via a patch pipette in the cell-attached mode from a cardiomyocyte at room temperature, showing the time courses of both variables after the application of FCCP (2 μM; filled bar). K^+ and Cl^- were the only charge carriers present and the cell was bathed in Ca^{2+}-free saline. The patch membrane was clamped at +20 mV. As there were multiple channels in the patch and a low sampling rate was used for this illustration, the activity of individual channels cannot be resolved from the trace illustrated. The time course of the corresponding channel open probability, NP_o, was analysed separately (at a higher sampling rate) for consecutive periods of 2·5 s (lower trace). *B*, NP_o is plotted as a function of the MgG signal during the rising phase of the response (before rigor). The channel activity only increased significantly after the MgG signal reached a plateau level.

new plateau level, at about 44 ± 6% (mean ± S.E.M., $n = 13$) of the resting signal (Fig. 4*A*). That the mitochondria were still intact is confirmed by the autofluorescence signal, which rather than the decrease expected on cellular permeabilization, increased (mean increase to 164 ± 16%, $n = 13$). The increase in NAD(P)H autofluorescence probably reflects inhibition of mitochondrial respiration. Further, application of the uncoupler FCCP after this degree of permeabilization resulted in the expected decrease of the autofluorescence signal (mean decrease to 68 ± 9%, $n = 3$; shown in Fig. 4*B*) associated with the depolarization of $\Delta\psi_m$ by the uncoupler, again indicating maintained mitochondrial function.

In the presence of 100 μM digitonin, the application of FCCP had no effect on the MgG signal (41 ± 5%, $n = 3$, before and after FCCP). This lack of effect suggests the absence of any significant extramitochondrial and/or intramitochondrial Mg^{2+} gradient, and is to be expected if our interpretation of the signal is correct, i.e. that it arises from ATP hydrolysis, given the supply of ATP and Mg^{2+} in the saline. Exposure to lower concentrations of digitonin (5–20 μM), which permeabilize only the plasma membrane (Roe *et al.* 1990), had similar effects, with a decrease of MgG fluorescence to 45 ± 8% ($n = 6$) and an increase of NAD(P)H autofluorescence to 144% ± 16 ($n = 6$). As there was no significant difference between these responses and those to 100 μM digitonin, which also permeabilizes the SR, these data suggest minimal dye-loading into the SR. Further exposure to 0·5% Triton X-100, which additionally permeabilizes mitochondrial membranes, led to complete loss of the remaining MgG signal to background levels ($n = 14$) and also to almost total loss of the autofluorescence signal (9 ± 10%, $n = 14$) (Fig. 4*A*). Thus, about 60% of the MgG signal is cytosolic, while up to 40% of the signal appears to originate from MgG localized to the mitochondria.

Since under control conditions, the intramitochondrial pH in rat myocytes will be about one pH unit more alkaline than that of the cytoplasm, and will equilibrate with that of the cytoplasm in the presence of the uncoupler FCCP (Reers, Kelly & Smith, 1989), the lack of effect of FCCP on the mitochondrial MgG fluorescence signal in the present study (see above) argues against any significant pH sensitivity of the dye. Furthermore, when cells were exposed to 10 mM NH_4Cl for 5 min to induce a period of alkalinization, which would be expected to leave a significant acid load on washout (e.g. Lagadic-Gossmann, Buckler & Vaughan-Jones, 1992), only minimal changes in MgG fluorescence were observed both during (112 ± 2%, $n = 4$) and after (109 ± 2%, $n = 4$) the NH_4Cl application (data not shown).

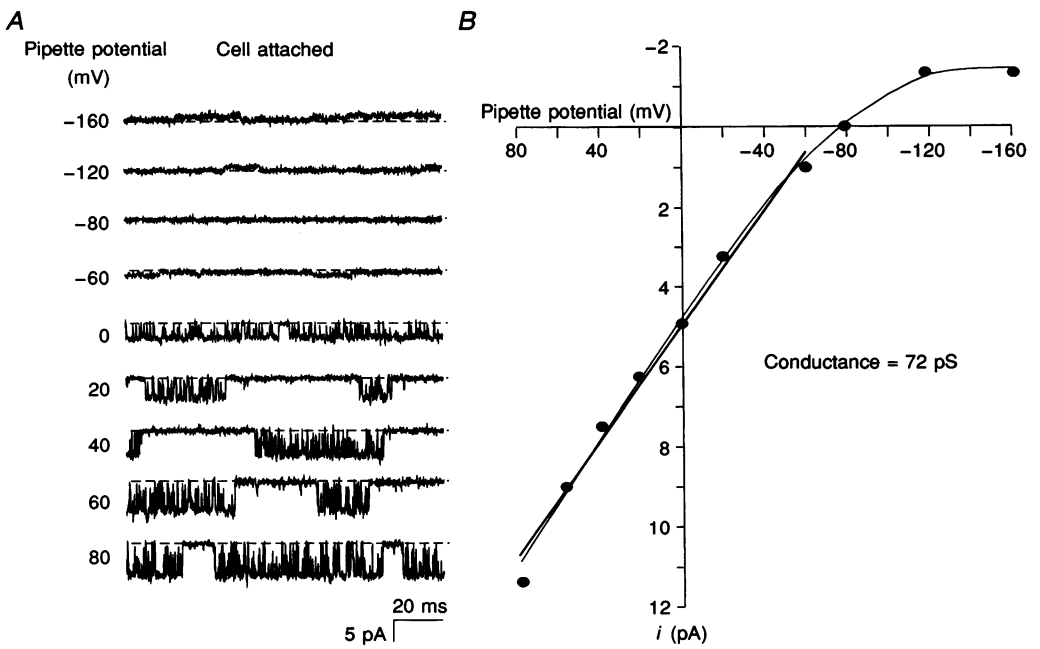

Figure 6. Properties of the single-channel current in the presence of FCCP

A, examples of single-channel activity recorded via a patch pipette in the cell-attached configuration from a cardiomyocyte bathed in Ca^{2+}-free saline at room temperature. The cell was also loaded with MgG. Once the MgG signal had reached a plateau after the addition of FCCP and channel activity was well established, the patch pipette potential was clamped at a range of potentials. In *B* the *i*–*V* curve is shown. The single-channel conductance was calculated by fitting a linear regression to the *i*–*V* curve over the range of patch pipette potentials from +60 to −60 mV. The properties of the single-channel current are all consistent with their identification as K_{ATP} channels.

K_{ATP} channels start to open as $[Mg^{2+}]_i$ reaches a plateau

In order to establish the correlation between changes in $[Mg^{2+}]_i$ and changes in K_{ATP} channel activity, cell-attached patch recordings were made simultaneously with MgG signals from myocytes bathed in Ca^{2+}-free saline. The omission of Ca^{2+} from the bath solution does not affect the single-channel current (Horie, Irisawa & Noma, 1987) but does help to exclude contamination of the records with Ca^{2+}-dependent K^+ channels.

Figure 5 illustrates the changes in single-channel activity in response to FCCP. Similar responses were observed in five other experiments. The patch membrane was clamped at +20 mV. Following application of FCCP, the MgG signal rose as described above, without any associated change in channel activity. The MgG signal then showed a secondary, slower increase towards a plateau during which there was a progressive increase in channel activity. The lower trace in Fig. 5*A* shows the time course of the change in channel open probability, NP_o (calculated for consecutive periods of 2·5 s). In Fig. 5*B*, NP_o is plotted as a function of the MgG signal (also averaged for consecutive periods of 2·5 s) up to the moment of cell shortening; it is clear that there was almost no significant channel activity until the MgG signal stabilized at about 190%. After cell shortening, indicated by the sudden decrease in MgG fluorescence towards a lower level, the channel activity further increased (see Fig. 5*A*).

Properties of K_{ATP} channels in cell-attached patch recordings

In many patches, some tonic activity of a small conductance channel was seen under resting (control) conditions. However, after metabolic inhibition (see below) or uncoupler, a larger conductance channel invariably appeared. In many patches, there were so many channels that it was difficult to resolve single-channel events. However in smaller patches, the properties of the single channels could be characterized. Once the MgG signal had reached a plateau and channel activity was well established, the patch membrane potential was clamped at a range of potentials, to characterize the *i–V* relationship for the single-channel current (Fig. 6*A* and *B*). The channels showed pronounced inward rectification, carrying only minimal outward current at depolarized membrane potentials. The single-channel conductance was calculated by fitting a linear regression to the *i–V* curve over the range of patch pipette potentials from +60 to −60 mV, giving a slope conductance of 69 ± 3 pS ($n = 5$). When the cells were additionally loaded with BAPTA AM, a similar conductance (73 ± 2 pS, $n = 3$) was found. These properties were all consistent with the identification of the channels as K_{ATP} channels (Horie *et al.* 1987).

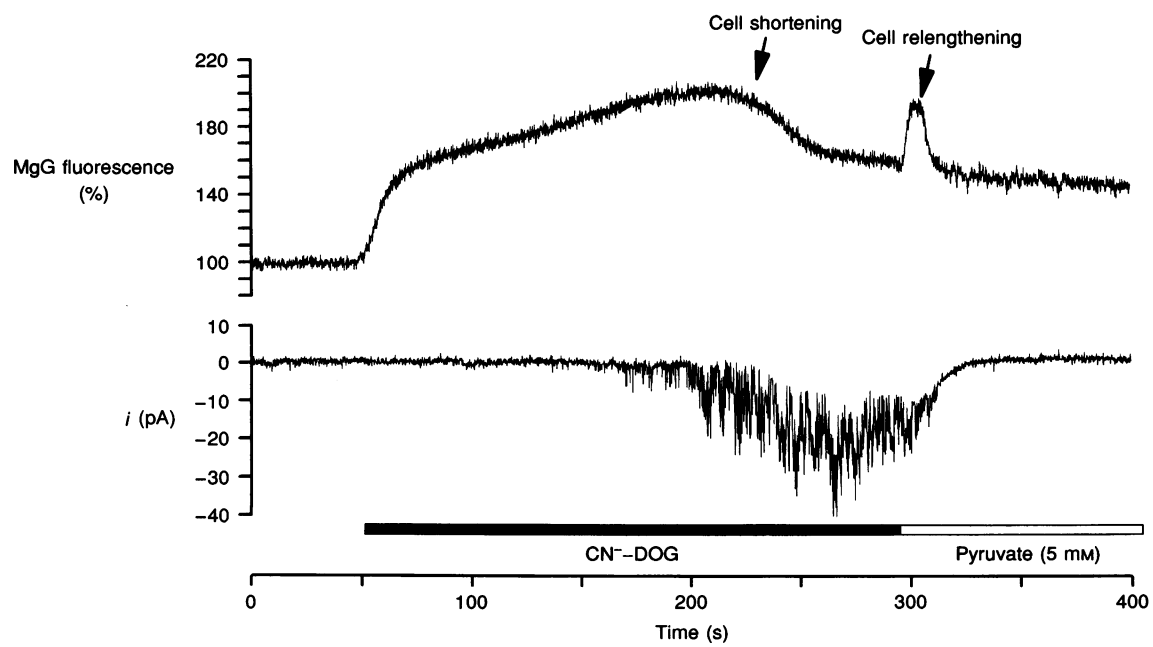

Figure 7. Time course of the changes in MgG fluorescence and K_{ATP} channel activity in the presence of CN^-–DOG and during reperfusion

Simultaneous measurement of MgG fluorescence (upper trace) and single-channel activity recorded in the cell-attached mode (lower trace) were recorded from a cardiomyocyte bathed in Ca^{2+}-free saline at 34 °C showing the different time course of both variables during and after the application of CN^- (2 mM) and DOG (20 mM) (CN^-–DOG; filled bar). Since DOG irreversibly inhibits glycolysis, pyruvate (5 mM) was added to the bath solution (open bar) on reperfusion. Similar recording conditions as described in Fig. 5.

Changes in $[Mg^{2+}]_i$, K_{ATP} channel activity, and $[Ca^{2+}]_i$ in response to the inhibition of mitochondrial respiration and glycolysis

The same set of variables were then examined during inhibition of both mitochondrial and glycolytic metabolism, using the now standard combination of CN^- and DOG. In response to this regime (at 34 °C) the MgG signal rose rather slowly to a value similar to that seen with FCCP (mean increase to 169 ± 4%, $n = 29$), again reaching a plateau just before the onset of rigor (mean time of shortening, 431 ± 35 s, $n = 29$).

Cell-attached patches were made in combination with MgG fluorescence measurements. In the example illustrated in Fig. 7, we recorded the membrane current in a large membrane patch containing multiple channels. Again, the activity of the K_{ATP} channels (mean single-channel conductance, 83 ± 2 pS, $n = 3$) increased only as the MgG signal reached a plateau ($n = 6$). After cell shortening, channel activity gradually started to decline. Since DOG irreversibly inhibits glycolysis, pyruvate was added to the bath solution during washout to provide mitochondrial substrate. On washout, the channel activity abruptly stopped before a substantial decrease in MgG fluorescence occurred, again demonstrating the different range of sensitivity of the two variables to changes in $[ATP]_i$.

Dual loading techniques were used to examine the relationship between the rise in MgG fluorescence, indicating cellular ATP depletion, and the rise in $[Ca^{2+}]_i$, during and after a period of metabolic inhibition, more precisely. In the present study, the qualitative sequence of reversible $[Ca^{2+}]_i$ and $[Mg^{2+}]_i$ changes was the same in cells that relengthened ($n = 5$, not shown) and cells that hypercontracted ($n = 8$, Fig. 8), except that $[Ca^{2+}]_i$ oscillations were often seen in hypercontracted cells. Thus, we consistently found that, after the application of CN^-–DOG, an initial rise in $[Ca^{2+}]_i$ occurred before cell shortening as the MgG fluorescence rose towards a plateau level. In the experiment shown here, following a delay after the onset of rigor, $[Ca^{2+}]_i$ rose further without any further change in MgG fluorescence. On washout of CN^-–DOG, reproduction of ATP led to hypercontracture, followed by some form of relaxation, possibly associated with the dramatic decrease of $[Ca^{2+}]_i$. Subsequently, oscillatory contractions coinciding with large $[Ca^{2+}]_i$ oscillations could be seen as small

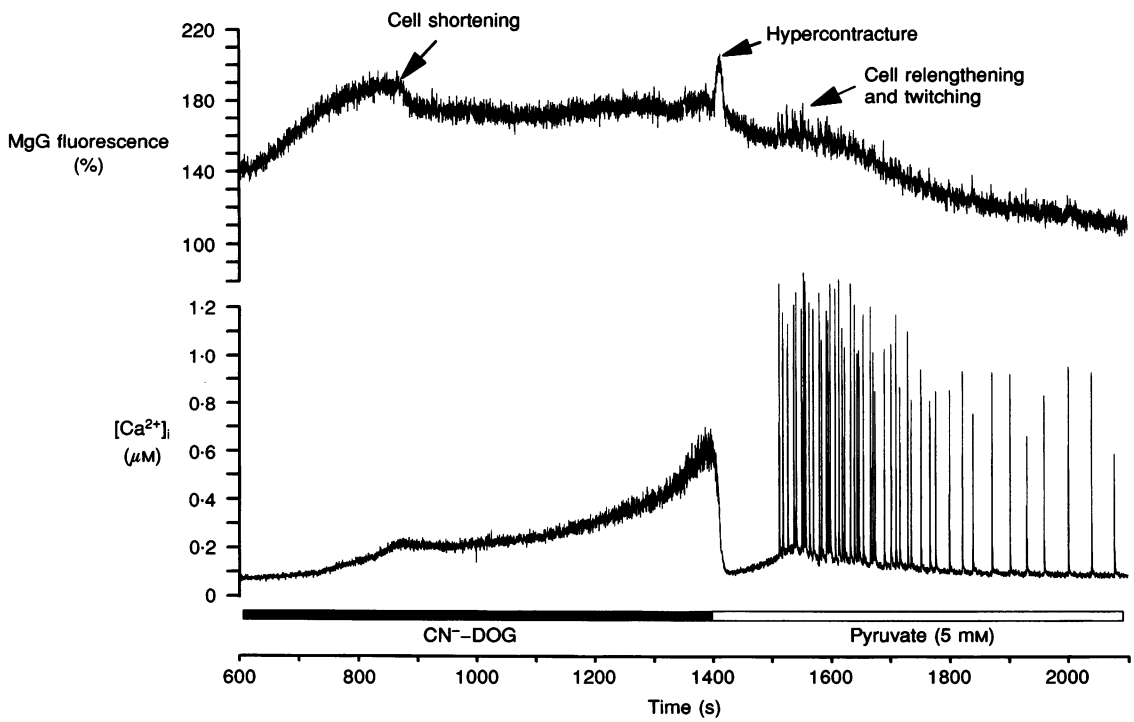

Figure 8. Time course of changes in MgG fluorescence and $[Ca^{2+}]_i$ in the presence of CN^-–DOG and during reperfusion

Fluorescence signals obtained from a cardiomyocyte loaded with both MgG (upper trace) and fura-2 (lower trace) showing the time course of MgG fluorescence in relation to changes in $[Ca^{2+}]_i$ during the application of CN^-–DOG (filled bar; concentration as in Fig. 7) and on reperfusion with the addition of pyruvate (5 mM; open bar). The early stages of the experiment are not shown. An initial rise in $[Ca^{2+}]_i$ occurred as the MgG signal reached a plateau. The MgG signal remained stable after cell shortening while $[Ca^{2+}]_i$ continued to rise. Reperfusion approximately 10 min after cell shortening instantaneously caused further cell shortening followed by relengthening as indicated, coincident with a rapid decrease in $[Ca^{2+}]_i$. The subsequent $[Ca^{2+}]_i$ oscillations were superimposed on the slow decrease of the MgG signal. The experiment was performed at 34 °C.

deflections of the MgG signal superimposed on the gradual decrease in MgG fluorescence. As $[Mg^{2+}]_i$ and $[Ca^{2+}]_i$ compete for intracellular binding sites (Murphy *et al.* 1989), $[Mg^{2+}]_i$ could be genuinely altered during large $[Ca^{2+}]_i$ fluctuations. Thus even under conditions in which the cardiomyocytes are severely $[Ca^{2+}]_i$ overloaded, changes in MgG fluorescence still primarily reflected changes in $[Mg^{2+}]_i$.

Changes in $[Mg^{2+}]_i$ and mitochondrial function during inhibition of mitochondrial respiration and glycolysis: role of the mitochondrial F_1F_0-ATPase in determining the rate of cellular ATP depletion

In a further attempt to correlate changes in $[Mg^{2+}]_i$ with changing mitochondrial function during metabolic inhibition and recovery, MgG fluorescence and NAD(P)H autofluorescence were measured simultaneously in response to CN^-–DOG (Fig. 9).

The inhibition of mitochondrial respiration by CN^- resulted in a rapid increase in NAD(P)H autofluorescence (mean increase to 155 ± 22%, $n = 6$). The MgG signal rose rather slowly (mean increase to 167 ± 6%, $n = 6$) reaching a plateau just before the onset of rigor (mean time to cell shortening, 540 ± 105 s, $n = 6$). Washout of CN^-–DOG resulted in a fast recovery and undershoot of the NAD(P)H autofluorescence. This was rapidly followed by cell relengthening and a slower recovery of the MgG signal.

The activity of the mitochondrial ATPase during the combined inhibition of mitochondrial respiration and glycolysis with CN^-–DOG was studied further by examining the rates of depolarization of $\Delta\psi_m$ before and after oligomycin (5 μg ml^{-1}). NAD(P)H autofluorescence was measured simultaneously as a control to assess the rate of inhibition of mitochondrial respiration by CN^-. This series of experiments was performed at room temperature. Under control conditions (Fig. 10*A*), after the application of CN^-–DOG, autofluorescence increased (mean increase to 239 ± 24%, $n = 4$), indicating inhibition of mitochondrial respiration by CN^-. The JC-1 signal (at 530 nm), however, changed very little reaching only about 10% change over a period of 60 s (mean increase to 111 ± 6%, $n = 4$). After application of oligomycin (Fig. 10*B*), the change in autofluorescence to CN^-–DOG was similar (mean increase to 228 ± 28%, $n = 4$), but now the JC-1 signal showed a much faster increase to a steady state of a roughly 70% increase after 60 s (mean increase to 168 ± 14%, $n = 4$). Figure 10*C*

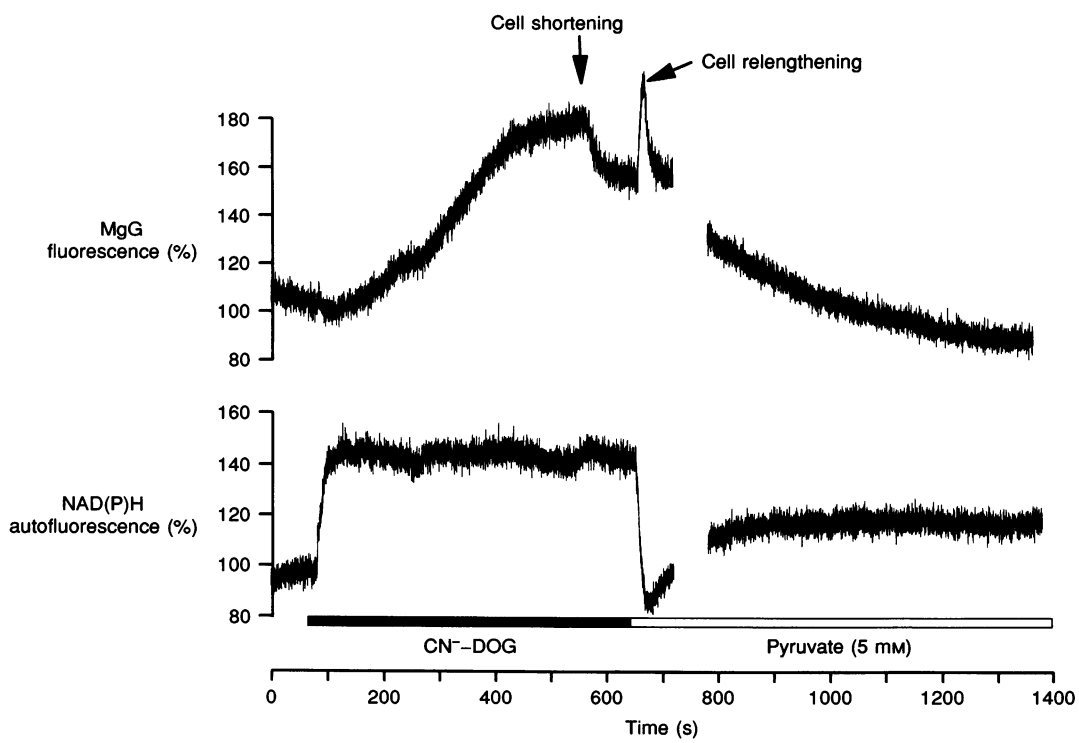

Figure 9. Time course of changes in MgG fluorescence and NAD(P)H autofluorescence in the presence of CN^-–DOG and during reperfusion

Simultaneous measurement of MgG fluorescence and NAD(P)H autofluorescence from a cardiomyocyte in response to CN^-–DOG (filled bar; concentration as in Fig. 7). Pyruvate (5 mM) was added to the bath solution on reperfusion (open bar). NAD(P)H autofluorescence increased rapidly following inhibition of respiration, and recovered promptly on washout in the presence of pyruvate. In contrast, both the increase of $[Mg^{2+}]_i$ and its recovery were very much slower. The slow decrease of MgG fluorescence on reperfusion corresponds with the slow recovery of NAD(P)H autofluorescence to a new steady state after an initial undershoot. The experiment was performed at 34 °C.

shows the change in NAD(P)H fluorescence as a function of the JC-1 signal in response to CN^-–DOG in the presence and absence of oligomycin, further illustrating the role of the ATPase in maintaining $\Delta\psi_m$.

The energetic costs of this mitochondrial ATPase activity can be deduced from the impact of oligomycin on the time course of the change in $[Mg^{2+}]_i$ to CN^-–DOG. Oligomycin, added to the bath solution 5 min prior to the addition of CN^-–DOG, had no significant effect on the increase in NAD(P)H autofluorescence (control of $232 \pm 39\%$, $n = 5$ and $180 \pm 22\%$, $n = 5$ in the presence of oligomycin). Similarly, the total rise in MgG fluorescence was not significantly altered by oligomycin (control $160 \pm 5\%$, $n = 7$ and in the presence of oligomycin, $180 \pm 22\%$,

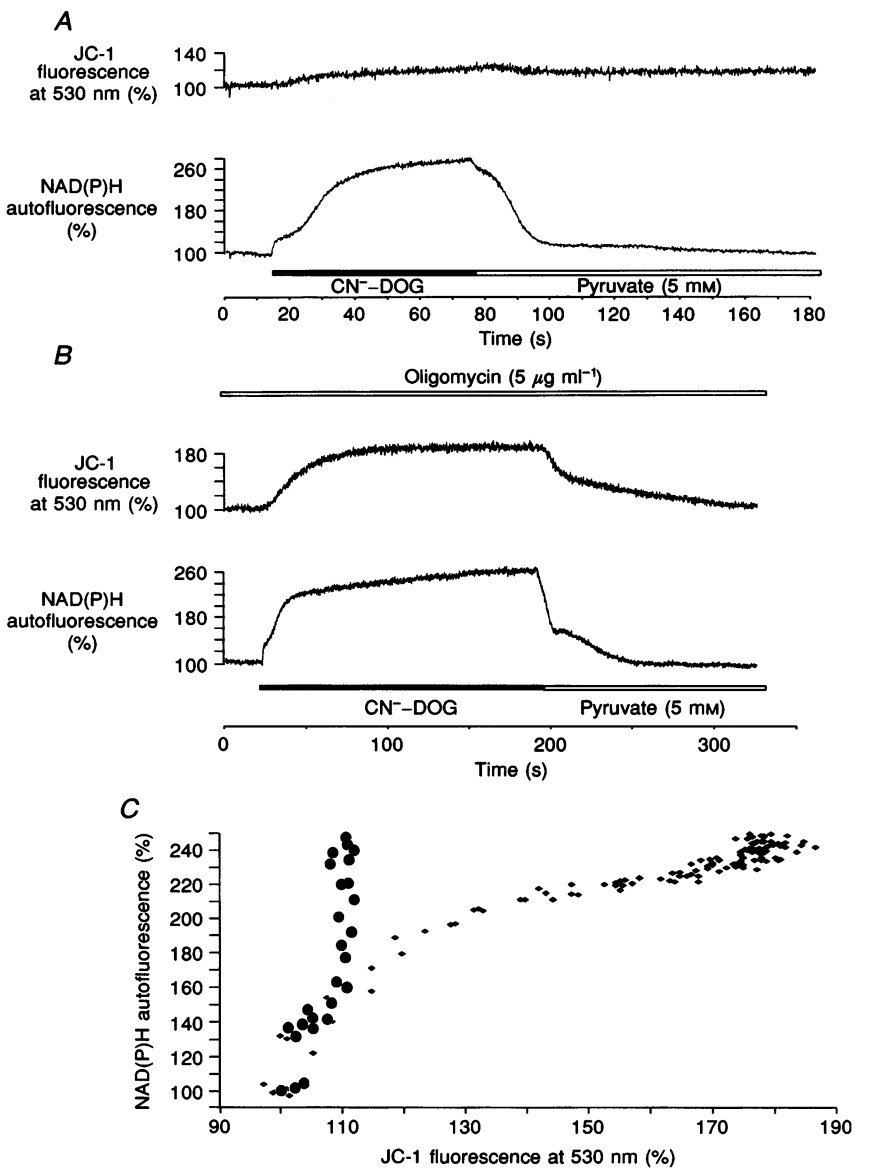

Figure 10. Relationship between changes in JC-1 fluorescence and NAD(P)H fluorescence in response to CN^-–DOG in the presence and absence of oligomycin

A and *B*, simultaneous measurements of JC-1 fluorescence (measured at 530 nm) (upper trace) and NAD(P)H autofluorescence (lower trace) from single cardiomyocytes. Pyruvate (5 mM; open bar) was added to the bath solution on washout of CN^-–DOG. Under control conditions (*A*), autofluorescence increased after inhibition of mitochondrial respiration by CN^-–DOG (filled bar; concentration as in Fig. 7). The JC-1 signal changed very little reaching only about 10% change over a period of 60 s. In the presence of oligomycin (5 μg ml^{-1}; *B*), the change in autofluorescence to CN^-–DOG was similar, but now the JC-1 signal showed a much faster increase to a steady state of a roughly 70% increase after 60 s. *C*, plot of the NAD(P)H fluorescence as a function of the JC-1 fluorescence during the onset of the response to CN^-–DOG in the presence (◆) and absence (●) of oligomycin.

$n = 7$). However, the half-time of the MgG rise was significantly increased from 575 ± 235 s ($n = 7$) to 1971 ± 357 s ($n = 7$). The lower rate of ATP depletion, reflected by the slower MgG rise, resulted in a significant delay of the development of rigor contracture: the time to shortening significantly increased from 881 ± 285 s ($n = 7$) to 2894 ± 447 s ($n = 7$). Thus in quiescent rat cardiomyocytes, during application of CN^-–DOG, the mitochondrial ATPase activity accelerates the depletion of the cellular ATP pool while serving to maintain $\Delta\psi_m$.

DISCUSSION

Properties of MgG as an indicator for changes in $[Mg^{2+}]_i$

In the present study, we examined the usefulness of the new probe MgG to monitor changes in $[Mg^{2+}]_i$ as a reflection of changes in $[ATP]_i$ in rat cardiomyocytes and to correlate these with changes in either $[Ca^{2+}]_i$ or mitochondrial function.

By dual loading cells with fura-2, it was clear that Ca^{2+} signals did not contribute significantly to the measurements of $[Mg^{2+}]_i$. The combined measurements also confirmed that changes in MgG fluorescence did not affect the fura-2 ratio and vice versa, excluding interaction between the two fluorescent indicators, always a potential hazard of using multiple dyes. Consistent with the properties of other Mg^{2+} indicators (Murphy *et al.* 1989; Silverman *et al.* 1994), we also found no significant pH effect on MgG fluorescence in these cells.

At the moment of cell shortening the MgG fluorescence consistently fell to a lower level. This could be an artefact due to changes in cell shape combined with possible non-linearities in the sensitivity of the photomultiplier tube over its window, and were not described in experiments using mag-indo-1 under similar conditions (Silverman *et al.* 1994). As an attempt to differentiate between true changes in $[Mg^{2+}]_i$ and movement artefacts we used 2,3-butanedione monoxime (BDM) which blocks myofibrillar cross-bridge cycling (Siegmund, Schlüter & Piper, 1993). However, in the presence of BDM, changes in cell shape on reperfusion were delayed but not inhibited (results not shown), and so these experiments failed unequivocally to clarify the issue. However, we consistently observed that the initial rise in MgG fluorescence at the moment of reperfusion preceded any changes in cell shape and occurred both on relengthening and on hypercontracture, suggesting a reflection of true changes in $[Mg^{2+}]_i$ which we cannot explain at present.

Measurements of $[Mg^{2+}]_i$ as an index of changing $[ATP]_i$

We have found that changes in $[Mg^{2+}]_i$ in response to inhibition or uncoupling of oxidative phosphorylation behave in full accord with the hypothesis that the changes arise from dissociation of Mg^{2+} from ADP following ATP hydrolysis. Permeabilizing the cells with digitonin showed that a significant proportion of the MgG signal originated from mitochondria (Fig. 4*A*). The same problem applies to the indicator mag-indo-1 (Silverman *et al.* 1994). However this does not seem to impair the usefulness of the indicators to follow changes in $[Mg^{2+}]_i$ during metabolic inhibition, perhaps partly because there does not appear to be a significant Mg^{2+} gradient between the cytosol and the mitochondria (Jung & Brierly, 1984).

Combined measurements of MgG fluorescence and K_{ATP} channel activity further served to clarify the relationship between changes in $[Mg^{2+}]_i$ and $[ATP]_i$. K_{ATP} channel activity was only prominent after the MgG signal reached a plateau level during metabolic inhibition and disappeared on reperfusion before any decrease in $[Mg^{2+}]_i$. This suggests that changes in $[Mg^{2+}]_i$ primarily reflect changes in the millimolar range, as $[ATP]_i$ falls from resting levels as high as 10 mM (Geisbuhler *et al.* 1984) and that the K_{ATP} channel activity registers changes in the submillimolar range, consistent with the estimated K_D for ATP for the channel of 20–100 μM (Noma, 1983; Lederer & Nichols, 1989).

It has been suggested that local [ATP] close to K_{ATP} channels may be governed primarily by local glycolytic activity and may differ significantly from global $[ATP]_i$ (Weiss & Lamp, 1989). Changes in MgG fluorescence will primarily reflect global changes in $[Mg^{2+}]_i$ and thus global $[ATP]_i$. Thus, one might anticipate that, during anoxia, glycolytically produced ATP in the vicinity of K_{ATP} channels may prevent opening of the channels despite a considerable decrease in global $[ATP]_i$, seen as an increase in $[Mg^{2+}]_i$. However, in the present experiments, either both glycolysis and respiration were inhibited (with CN^-–DOG) or mitochondrial ATP consumption in the presence of uncoupler was so effective that this functional ATP compartmentalization was probably not an important issue in our experiments.

At first sight our data seem to contradict the observation that the failure of electrically stimulated contraction in response to glucose-free anoxia, associated with an increased K^+ conductance and the shortening of the action potential (Stern *et al.* 1988), occurs before any significant rise in $[Mg^{2+}]_i$ (Silverman *et al.* 1994). However, NMR studies have shown that the action potential shortens before there is any substantial fall of total tissue [ATP] (Elliott, Smith & Allen, 1989). In addition, because of its relatively large conductance and the large number of channels on the myocyte membrane, a very small increase in channel opening probability, too small to be seen in the present single-channel records, may have major effects on cell conductance and action potential duration (Nichols, Ripoll & Lederer, 1991). Thus given a $K_{D(ATP)}$ of 20–100 μM and the binding capacity of intracellular ligands for an unknown fraction of liberated Mg^{2+} (Murphy *et al.* 1989), it is still possible for a small decrease in $[ATP]_i$ to result in a significant decrease in action potential duration and contractile failure without having a measurable effect on $[Mg^{2+}]_i$.

Magnesium also affects K_{ATP} channel activity directly. In isolated patches (Findlay, 1987) and in cell-attached patches recorded from internally permeabilized cardiac myocytes (Horie *et al.* 1987), Mg^{2+} applied at the cytosolic side of the plasmamembrane reduced both the amplitude and the activity of K_{ATP} channels for outwardly directed currents in a dose-dependent manner. Thus, the inward rectification of the current–voltage relationship of the single-channel K_{ATP} current may be related to the rise in $[Mg^{2+}]_i$ observed in the present experiments during ATP depletion. However, the rundown of the K_{ATP} channel observed after the development of rigor, involving dephosphorylation of the K^+ channel protein, is Ca^{2+} but not Mg^{2+} dependent (Findlay, 1987).

Combined measurements of $[Mg^{2+}]_i$ and parameters of mitochondrial function during metabolic inhibition: role of the mitochondrial ATPase activity as a determinant of the rate of ATP depletion

Simultaneous measurements of NAD(P)H autofluorescence and measurements of either $\Delta\psi_m$ or $[Mg^{2+}]_i$ offer further insight into the mechanisms regulating mitochondrial ATP production within the cell. Mitochondrial depolarization by FCCP increases the rate of oxidation of NAD(P)H (Figs 2 and 3*A*). The depolarization of $\Delta\psi_m$ also promotes reversal of the mitochondrial ATPase which rapidly depletes cellular ATP supplies (see Fig. 3*A*). As soon as $\Delta\psi_m$ is restored on washout of FCCP, cellular ATP levels recover and the activity of the respiratory chain will return to its original level (Fig. 3*A*). The inhibition of the mitochondrial ATPase with oligomycin prevented ATP hydrolysis but not the increased rate of oxidation (Fig. 3*B*), showing that stimulation of respiration is a response to the depolarization of $\Delta\psi_m$ and not to a decrease in the [ATP] : [ADP] ratio.

With blockade of the electron transport chain with CN^-, the NADH : NAD^+ ratio rises and $\Delta\psi_m$ cannot be sustained in the face of leaks (Duchen *et al.* 1993; Di Lisa *et al.* 1995). In these circumstances the maintenance of $\Delta\psi_m$ is effected by the mitochondrial ATP synthase, which reverses and acts as a proton translocating ATPase. This mechanism for preservation of $\Delta\psi_m$ can be abolished by inhibiting the mitochondrial ATPase activity with oligomycin (Fig. 10). The rate of ATP depletion will be dependent on the combined activity of ATP consuming processes. During glucose-free anoxia both in quiescent (Duchen *et al.* 1993) and in electrically stimulated cardiomyocytes (Di Lisa *et al.* 1995) $\Delta\psi_m$ only fully depolarized after development of rigor. In electrically stimulated cells, oligomycin accelerated the depolarization of $\Delta\psi_m$ during anoxia without development of asystole or rigor, while the combined inhibition of glycolysis and mitochondrial respiration (iodoacetate and rotenone, respectively) resulted in the rapid dissipation of $\Delta\psi_m$ and the development of rigor (Di Lisa *et al.* 1995). This suggested that reversal of the mitochondrial ATPase can serve to maintain the mitochondrial potential at the expense of glycolytically produced ATP.

In the present study, the presence of DOG prevented glucose utilization. The combination of CN^- and DOG therefore restricted the cytosolic ATP pool to the existing cellular levels of $[ATP]_i$ and creatine phosphate. In quiescent cardiomyoctes, the role of mitochondrial ATPase activity in depleting ATP during metabolic inhibition will not be masked by a significant ATP consumption by actomyosin and other ATPases, i.e. Na^+–K^+-ATPase and sarcoplasmic and plasmalemmal Ca^{2+}-ATPases. In the present study, we demonstrate that under these conditions oligomycin has a dramatic effect in slowing ATP consumption during metabolic inhibition. Although oligomycin also inhibits sarcolemmal Na^+–K^+-ATPase at higher concentrations (Fahn, Koval & Albers, 1966), this is unlikely to contribute to our data. Inhibition of the Na^+–K^+ pump in quiescent cardiomyocytes causes spontaneous activity and hypercontracture due to $[Ca^{2+}]_i$ overload (Hayashi *et al.* 1994), while in hypoxic ferret papillary muscles inhibition of the Na^+–K^+ pump with ouabain causes an increase in $[Na^+]_i$ and $[Ca^{2+}]_i$ (Guarnieri, 1987). In our experiments, however, the cells remained rod shaped and quiescent in the presence of oligomycin. Furthermore, these events would result in an increase, rather than a decrease of the rate of ATP depletion. Therefore the energy-saving effects of oligomycin observed in the present study are attributable to an inhibition of the mitochondrial ATPase. Thus together with earlier reports (Haworth *et al.* 1981; Noll, Koop & Piper, 1992; Di Lisa *et al.* 1995), our observations point to the mitochondrial ATPase as a major determinant of ATP hydrolysis in the anoxic or metabolically stressed myocardium of the rat.

The depletion of ATP during inhibition of mitochondrial respiration results in rigor. On reperfusion, activity of the respiratory chain restores $\Delta\psi_m$, and permits mitochondrial ATP production. The undershoot of NAD(P)H signals on reperfusion most probably reflects accumulation of ADP during the preceding period (Fig. 9). On reoxygenation, ADP stimulates mitochondrial synthase activity (Chance & Williams, 1956); the increased proton flux will depolarize $\Delta\psi_m$, increasing the respiratory rate and thus the rate of oxidation of NADH. The relationship between increased mitochondrial synthase activity and changes in NAD(P)H autofluorescence was also suggested by White & Wittenberg (1995) in paced cardiomyocytes. This explanation for the undershoot of the NAD(P)H autofluorescence is further supported by the temporal correlation between the recovery of the undershoot and the restoration of $[Mg^{2+}]_i$ to resting levels, which in turn indicates a recovery of the $[ATP]_i$: $[ADP]_i$ ratio.

Relationship between changes in $[Mg^{2+}]_i$, reflecting changes in $[ATP]_i$ and $[Ca^{2+}]_i$: a synthesis

As changes in $[Mg^{2+}]_i$ and $[Ca^{2+}]_i$ can be monitored simultaneously in single cells dual loaded with both MgG and fura-2, it is possible to correlate changes in $[Ca^{2+}]_i$ with

changes in $[Mg^{2+}]_i$, and thus with changes in $[ATP]_i$ during and following periods of metabolic inhibition. $[Ca^{2+}]_i$ rises significantly after the onset of energy-dependent rigor contracture (Miyata *et al.* 1992). In accordance with an earlier report by Eisner, Nichols, O'Neill, Smith & Valdeolmillos (1989), we found that following glycolytic and mitochondrial inhibition $[Ca^{2+}]_i$ rose prior to cell shortening. This $[Ca^{2+}]_i$ rise took place as $[Mg^{2+}]_i$ rose towards a plateau level, thus as $[ATP]_i$ had begun to fall (Fig. 8). The early rise in $[Ca^{2+}]_i$ has been attributed, via Na^+–Ca^{2+} exchange, to a rise in $[Na^+]_i$, itself secondary to Na^+–H^+ exchange stimulated by intracellular acidification. A rise in $[Na^+]_i$ may also result from inhibition of the Na^+–K^+-ATPase as $[ATP]_i$ falls (Donoso, Mill, O'Neill & Eisner, 1992; Katoh, Satoh, Nakamura, Terada & Hayashi, 1994). After a variable delay, $[Ca^{2+}]_i$ then rose continuously following complete ATP depletion.

The outcome on reperfusion was largely dependent on the $[Ca^{2+}]_i$ load during the preceding ischaemic period (see Siegmund *et al.* 1993). On reperfusion, cells either partially relengthened, retaining their rectangular shape, or they rapidly crushed into rounded blebbed forms with an absent sarcomere pattern and disordered myofibrils (hypercontracture). In the latter case, they often displayed contractile and $[Ca^{2+}]_i$ oscillations. Both in relengthened and hypercontracted cells, $[ATP]_i$ at least partially recovers (Bowers *et al.* 1993). We found that $[Mg^{2+}]_i$ decreased on reperfusion in both relengthened and hypercontracted cells and at least partially recovered towards its intitial value (see also Di Lisa *et al.* 1995). However, the recovery of $[Mg^{2+}]_i$ was slow. This is consistent with parallel experiments in whole heart (Murphy *et al.* 1989), which demonstrated that the gradual decrease in $[Mg^{2+}]_i$ was associated with a gradual increase in $[ATP]_i$. In cultured rat hepatocytes, similar experiments showed that the slow decrease in $[Mg^{2+}]_i$ on reperfusion was accompanied by a slow increase in $[ATP]_i$, and a concomitant decrease in $[ADP]_i$ and $[AMP]_i$ (Harman, Nieminen, Lemasters & Herman, 1990). In the present study, $[Mg^{2+}]_i$ did not always recover to its control level, even after 20 min of reperfusion (results not shown). This is probably related to the loss of nucleotides from the cell following ATP breakdown (Reimer, Hill & Jennings, 1981). The qualitative sequence of reversible $[Ca^{2+}]_i$ and $[Mg^{2+}]_i$ changes was the same in cells that relengthened (not shown) and cells that hypercontracted, with the exception of oscillatory activity which was seen predominantly in hypercontracted cells during reperfusion. Thus $[Ca^{2+}]_i$ fell within 1 min to control levels, probably due to uptake by the sarcoplasmic reticulum (see Miyata *et al.* 1992). This fall in $[Ca^{2+}]_i$, which is possibly responsible for the (hardly noticeable) relaxation of hypercontracted cells, was never associated with a concomitant substantial decrease in $[Mg^{2+}]_i$. The undershoot of the NAD(P)H autofluorescence on reperfusion (see above) also suggests that full ATP recovery is comparatively delayed. The abolition of K_{ATP} channel activity preceding changes in cell shape on reperfusion (Fig. 7) on the other hand reflects an initial recovery of $[ATP]_i$ within the submillimolar range. In luciferase-injected cardiomyocytes, Bowers *et al.* (1993) observed that hypercontracture of the cells starts at around 100 μM ATP.

Thus, these observations together suggest that only a partial recovery of $[ATP]_i$ is needed for the events taking place in the early stages of reperfusion, i.e. for the relief of rigor contracture and subsequent relaxation (relengthening) or activation (hypercontracture) of the contractile elements and for the Ca^{2+} uptake by the sarcoplasmic Ca^{2+}-ATPase. Furthermore our experiments demonstrate that, while $[Mg^{2+}]_i$ has not yet recovered, huge $[Ca^{2+}]_i$ oscillations, probably involving Ca^{2+} release and re-uptake by a Ca^{2+} overloaded sarcoplasmic reticulum, can take place on reperfusion despite the reported interference of Mg^{2+} with the Ca^{2+} release channel of the sarcoplasmic reticulum (Meissner & Henderson, 1987). Although cells remained hypercontracted, the oscillatory activity usually gradually decreased; this was associated with the further recovery of diastolic $[Ca^{2+}]_i$ and of $[Mg^{2+}]_i$, indicating the restoration of cellular energy levels and $[Ca^{2+}]_i$ homeostasis.

Bowers, K. C., Allshire, A. P. & Cobbold, P. H. (1993). Continuous measurement of cytoplasmic ATP in single cardiomyocytes during simulation of the 'oxygen paradox'. *Cardiovascular Research* **27**, 1836–1839.

Chance, B. & Williams, G. R. (1956). The respiratory chain and oxidative phosphorylation. *Advances in Enzymology* **17**, 65–134.

Di Lisa, F., Blank, P. S., Colonna, R., Gambassi, G., Silverman, H. S., Stern, M. D. & Hansford, D. (1995). Mitochondrial membrane potential in single living adult rat cardiac myocytes exposed to anoxia or metabolic inhibition. *Journal of Physiology* **486**, 1–13.

Donoso, P., Mill, J. G., O'Neill, S. C. & Eisner, D. A. (1992). Fluorescence measurements of cytoplasmic and mitochondrial sodium concentration. *Journal of Physiology* **448**, 493–509.

Duchen, M. R., McGuinness, O., Brown, L. A. & Crompton, M. (1993). On the involvement of a cyclosporin A sensitive mitochondrial pore in myocardial reperfusion injury. *Cardiovascular Research* **27**, 1790–1794.

Eisner, D. A., Nichols, C. G., O'Neill, S. C., Smith, G. L. & Valdeolmillos, M. (1989). The effects of metabolic inhibition on intracellular calcium and pH in isolated rat ventricular myocytes. *Journal of Physiology* **411**, 393–418.

Elliott, A. C., Smith, G. L. & Allen, D. G. (1989). Simultaneous measurements of action potential duration and intracellular ATP in isolated ferret hearts exposed to cyanide. *Circulation Research* **64**, 583–591.

Eng, J., Lynch, R. M. & Balaban, R. S. (1989). Nicotinamide adenine nucleotide fluorescence spectroscopy and imaging of isolated cardiac myocytes. *Biophysical Journal* **55**, 621–630.

Fahn, S., Koval, G. J. & Albers, R. J. (1966). Sodium-potassium-activated triphosphate of *Electrophorus* electric organ. I. An associated sodium-activated transphosphorylation. *Journal of Biological Chemistry* **241**, 1882–1889.

FINDLAY, I. (1987). ATP-sensitive K^+ channels in rat ventricular myocytes are blocked and inactivated by internal divalent cations. *Pflügers Archiv* **410**, 313–320.

GEISBUHLER, T., ALTSCHULD, R. A., TREWYN, R., ANSEL, A. Z., LAMKA, K. & BRIERLY, G. P. (1984). Adenine nucleotide metabolism and compartmentalisation in isolated adult rat heart cells. *Circulation Research* **54**, 536–546.

GRYNKIEWICZ, G., POENIE, M. & TSIEN, R. Y. (1985). A new generation of Ca^{2+} indicators with greatly improved fluorescence properties. *Journal of Biological Chemistry* **260**, 3440–3450.

GUARNIERI, T. (1987). Intracellular sodium–calcium dissociation in early contractile failure in hypoxic ferret papillary muscles. *Journal of Physiology* **388**, 449–465.

HARMAN, A. W., NIEMINEN, A., LEMASTERS, J. J. & HERMAN, B. (1990). Cytosolic free magnesium, ATP and blebbing during chemical hypoxia in cultured rat hepatocytes. *Biochemical and Biophysical Research Communications* **170**, 477–483.

HAWORTH, R. A., HUNTER, D. R. & BERKOFF, H. A. (1981). Contracture in isolated adult rat heart cells. Role of Ca^{2+}, ATP, and compartmentation. *Circulation Research* **49**, 1119–1128.

HAYASHI, H., SATOH, H., NODA, N., TERADA, H., HIRANO, M., YAMASHITA, Y., KOBAYASHI, A. & YAMAZAKI, N. (1994). Simultaneous measurement of intracellular Na^+ and Ca^{2+} during K^+-free perfusion in isolated myocytes. *American Journal of Physiology* **266**, C416–422.

HORIE, M., IRISAWA, H. & NOMA, A. (1987). Voltage-dependent magnesium block of adenosine-triphosphate-sensitive potassium channel in guinea-pig ventricular cells. *Journal of Physiology* **387**, 251–272.

JUNG, D. W. & BRIERLY, G. P. (1994). Magnesium transport by mitochondria. *Journal of Bioenergetics and Biomembranes* **26**, 527–535.

KATOH, H., SATOH, H., NAKAMURA, T., TERADA, H. & HAYASHI, H. (1994). The role of Na^+/H^+ exchange and the Na^+/K^+ pump in the regulation of $[Na^+]_i$ during metabolic inhibition in guinea pig myocytes. *Biochemical and Biophysical Research Communications* **203**, 93–98.

KIRKELS, J. H., VAN ECHTFELD, C. J. H. & RUIGROK, T. J. C. (1989). Intracellular magnesium during myocardial ischemia and reperfusion: possible consequences for postischemic recovery. *Journal of Molecular and Cellular Cardiology* **21**, 1209–1218.

LAGADIC-GOSSMANN, D., BUCKLER, K. J. & VAUGHAN-JONES, R. D. (1992). Role of bicarbonate in pH recovery from intracellular acidosis in the guinea-pig ventricular myocyte. *Journal of Physiology* **458**, 361–384.

LEDERER, W. J. & NICHOLS, C. G. (1989). Nucleotide modulation of the activity of rat heart ATP-sensitive K^+ channels in isolated membrane patches. *Journal of Physiology* **419**, 193–212.

LEYSSENS, A. & DUCHEN, M. R. (1994). Changes in intracellular free magnesium with ATP depletion in single isolated rat cardiomyocytes. *Journal of Physiology* **480.P**, 90*P*.

LEYSSENS, A., NOWICKY, A. V., PATTERSON, L., CROMPTON, M. & DUCHEN, M. R. (1995). Changes in intracellular magnesium and ATP-regulated K^+ channel activity with changing metabolic state in isolated rat cardiomyocytes. *Journal of Physiology* **483.P**, 9*P*.

MEISSNER, G. & HENDERSON, J. S. (1987). Rapid calcium release from cardiac sarcoplasmic reticulum vesicles is dependent on Ca^{2+} and is modulated by Mg^{2+}, adenine nucleotide, and calmodulin. *Journal of Biological Chemistry* **262**, 3065–3073.

MIYATA, H., LAKATTA, E. G., STERN, M. D. & SILVERMAN, H. S. (1992). Relation of mitochondrial and cytosolic free calcium to cardiac myocyte recovery after exposure to anoxia. *Circulation Research* **71**, 605–613.

MURPHY, E., STEENBERGEN, C., LEVY, L. A., RAJU, B. & LONDON, R. E. (1989). Cytosolic free magnesium levels in ischemic rat heart. *Journal of Biological Chemistry* **264**, 5622–5627.

NAZARETH, W., YAFEI, N. & CROMPTON, M. (1991). Inhibition of anoxia-induced injury in heart myocytes by cyclosporin A. *Journal of Molecular and Cellular Cardiology* **23**, 1351–1354.

NICHOLS, C. G., RIPOLL, C. & LEDERER, W. J. (1991). ATP-sensitive potassium channel modulation of the guinea-pig ventricular action potential and contraction. *Circulation Research* **68**, 280–287.

NOLL, T., KOOP, A. & PIPER, M. (1992). Mitochondrial ATP-synthase activity in cardiomyocytes after aerobic-anaerobic metabolic transition. *American Journal of Physiology* **262**, C1297–1303.

NOMA, A. (1983). ATP-regulated K channels in cardiac muscle. *Nature* **305**, 147–148.

REERS, M., KELLY, R. A. & SMITH, T. W. (1989). Calcium and proton activities in rat cardiac mitochondria. Effect of matrix environment on behaviour of fluorescent probes. *Biochemical Journal* **257**, 131–142.

REERS, M., SMITH, T. W. & CHEN, L. B. (1991). J-aggregate formation of a carbocyanine as a quantitative fluorescent indicator of membrane potential. *Biochemistry* **30**, 4480–4486.

REIMER, K. A., HILL, M. L. & JENNINGS, R. B. (1981). Prolonged depletion of ATP and of the adenine nucleotide pool due to delayed resynthesis of adenine nucleotides following reversible myocardial ischemic injury in dogs. *Journal of Molecular and Cellular Cardiology* **13**, 229–239.

ROE, M. W., LEMASTERS, J. J. & HERMAN, B. (1990). Assessement of fura-2 for measurements of cytosolic free calcium. *Cell Calcium* **11**, 63–73.

SIEGMUND, B., SCHLÜTER, K.-D. & PIPER, H. M. (1993). Calcium and the oxygen paradox. *Cardiovascular Research* **27**, 1778–1783.

SILVERMAN, H. S., DI LISA, F., HUI, R. C., MIYATA, H., SOLLOTT, S. J., HANSFORD, R. G., LAKATTA, E. G. & STERN, M. D. (1994). Regulation of intracellular free Mg^{2+} in single adult mammalian cardiac myocytes. *American Journal of Physiology* **266**, C222–233.

STERN, M. D., SILVERMAN, H. S., HOUSER, S. G., JOSEPHSON, R. A., CAPROGOSSI, M. C., NICHOLS, C. G., LEDERER, W. J. & LAKATTA, E. G. (1988). Anoxic contractile failure in rat heart myocytes is caused by failure of intracellular Ca release due to alteration of the action potential. *Proceedings of the National Academy of Sciences of the USA* **85**, 6954–6958.

WEISS, J. N. & LAMP, S. T. (1989). Cardiac ATP-sensitive K^+channels. Evidence for preferential regulation by glycolysis. *Journal of General Physiology* **94**, 911–935.

WHITE, R. L. & WITTENBERG, B. A. (1995). Effects of calcium on mitochondrial NAD(P)H in paced rat ventricular myocytes. *Biophysical Journal* **69**, 2790–2799.

Acknowledgements

The work described in this study was supported by The British Heart Foundation and Action Research.

Author's present address

A. Leyssens: Departmente Medische Basiswetenschappen, Limburgs Universitair Centrum, Universitaire Campus, 3590 Diepenbeek, Belgium.

Author's email address

M. R. Duchen: m.duchen@ucl.ac.uk

Received 25 January 1996; accepted 18 June 1996.